


## RESEARCH ARTICLE

# Microglia actively remove NR1 autoantibody-bound NMDA receptors and associated post-synaptic proteins in neuron microglia co-cultures

Kazi Atikur Rahman<sup>1,2,3</sup>  | Marta Orlando<sup>1,2</sup> | Ayub Boulos<sup>4</sup> | Ewa Andrzejak<sup>5</sup> | Dietmar Schmitz<sup>1,2,3,5,6,7</sup> | Noam E. Ziv<sup>4</sup> | Harald Prüss<sup>1,5,8</sup> | Craig C. Garner<sup>1,2,5</sup> | Aleksandra Ichkova<sup>5</sup>

<sup>1</sup>Corporate Member of Freie Universität Berlin, Humboldt-Universität Berlin and Berlin Institute of Health, Neuroscience Research Center, Charité-Universitätsmedizin Berlin, Berlin, Germany

<sup>2</sup>Corporate Member of Freie Universität Berlin, Humboldt-Universität Berlin and Berlin Institute of Health, NeuroCure Cluster of Excellence, Charité-Universitätsmedizin Berlin, Berlin, Germany

<sup>3</sup>Corporate Member of Freie Universität Berlin, Humboldt-Universität Berlin and Berlin Institute of Health, Einstein Center for Neuroscience, Charité-Universitätsmedizin Berlin, Berlin, Germany

<sup>4</sup>Technion Faculty of Medicine, Rappaport Institute and Network Biology Research Laboratories, Haifa, Israel

<sup>5</sup>German Center for Neurodegenerative Diseases (DZNE) Berlin, Berlin, Germany

<sup>6</sup>Bernstein Center for Computational Neuroscience, Humboldt-Universität zu Berlin, Berlin, Germany

<sup>7</sup>Max Delbrück Center for Molecular Medicine in the Helmholtz Association, Berlin, Germany

<sup>8</sup>Corporate Member of Freie Universität Berlin, Humboldt-Universität Berlin and Berlin Institute of Health, Department of Neurology and Experimental Neurology, Charité-Universitätsmedizin Berlin, Berlin, Germany

## Correspondence

Aleksandra Ichkova, German Center for Neurodegenerative Diseases (DZNE) Berlin, 10117 Berlin, Germany.  
Email: [aleksandra.ichkova@dzne.de](mailto:aleksandra.ichkova@dzne.de)

Craig C. Garner, Charité-Universitätsmedizin Berlin, corporate member of Freie Universität Berlin, Humboldt-Universität Berlin and Berlin Institute of Health, Neuroscience Research Center, 10117 Berlin, Germany.  
Email: [craig.garner@charite.de](mailto:craig.garner@charite.de)

## Funding information

Bundesministerium für Bildung und Forschung, Grant/Award Numbers: 01GM1908D, 01GQ1420B; Deutsche Forschungsgemeinschaft, Grant/Award Numbers: 184695641, 327654276, 415914819, 431572356; Deutsches Zentrum für Neurodegenerative Erkrankungen; Einstein Stiftung Berlin; Germany's Excellence Strategy, Grant/Award Numbers: Exc-2049-390688087, PR1274/3-1, PR1274/4-1, PR1274/5-1; H2020 European Research Council, Grant/Award Number: 810580; Helmholtz-Gemeinschaft, Grant/Award Number: HIL-A03

## Abstract

Autoantibodies against the NR1 subunit of NMDA receptors (NMDARs) have been shown to promote crosslinking and internalization of bound receptors in NMDAR encephalitis (NMDARE). This internalization-mediated loss of NMDARs is thought to be the major mechanism leading to pathogenic outcomes in patients. However, the role of bound autoantibody in engaging the resident immune cells, microglia, remains poorly understood. Here, using a patient-derived monoclonal NR1 autoantibody (hNR1-mAb) and a co-culture system of microglia and neurons, we could show that hNR1-mAb bound to hippocampal neurons led to microglia-mediated removal of hNR1-mAb bound NMDARs. These complexes were found to accumulate inside endo-lysosomal compartments of microglia. Utilizing another patient isolated monoclonal autoantibody, against the  $\alpha 1$ -subunit of GABA<sub>A</sub> receptors ( $\alpha 1$ -GABA<sub>A</sub>-mAb), such removal of receptors was found to be specific to the antibody-bound receptor targets. Interestingly, along with receptor removal, we also observed a reduction in synapse number, more specifically in the numbers of post-synaptic proteins like PSD95 and Homer 1, when microglia were present in the culture. Importantly, mutations in the Fc region of hNR1-mAb,

This is an open access article under the terms of the [Creative Commons Attribution-NonCommercial](https://creativecommons.org/licenses/by-nc/4.0/) License, which permits use, distribution and reproduction in any medium, provided the original work is properly cited and is not used for commercial purposes.

© 2023 The Authors. GLIA published by Wiley Periodicals LLC.

blocking its Fc $\gamma$  receptor (Fc $\gamma$ R) and complement binding, attenuated hNR1-mAb driven loss of NMDARs and synapses, indicating that microglia engagement by bound hNR1-mAb is critical for receptor and synapse loss. Our data argues for an active involvement of microglia in removal of NMDARs and other receptors in individuals with autoimmune encephalitis, thereby contributing to the etiology of these diseases.

#### KEYWORDS

antibody mediated autoimmune encephalitis; autoantibodies; microglia, hippocampal neurons, co-culture, pre-labeling; NMDAR

## 1 | INTRODUCTION

NMDA receptor encephalitis (NMDARE), initially described as a paraneoplastic syndrome, is a neuro autoimmune disorder where autoantibodies are formed, most commonly, against NR1 subunit of NMDA receptor (NMDAR) (Josep Dalmau et al., 2007). NMDARE patients show myriad of symptoms including psychosis, impaired consciousness, behavioral changes (Day et al., 2011) autonomic dysfunction and catatonia (Barry et al., 2011; Josep Dalmau et al., 2019; Prüss, 2021). The mechanism of action of NR1 autoantibodies was reported to be receptor crosslinking by bound autoantibody, leading to internalization of receptor antibody complexes thereby reducing the number of NR1 positive NMDAR from the surface of neurons (Hughes et al., 2010). The crosslinking of receptors by bound antibody was shown to be mediated by Fc region of the autoantibody (Hughes et al., 2010). This crosslinking dependent receptor internalization was not observed when F(ab) fragments of NR1 reactive autoantibody, which lacks the Fc region, was bound to NMDARs on cultured hippocampal neurons (Hughes et al., 2010).

Apart from receptor crosslinking by bound antibody, Fc regions of sub-types of antibodies (IgG1, IgG3, among others) are also known to mediate downstream immune responses including binding to Fc receptors (FcRs) present on cells of monocytic lineage and antigen presenting cells (APCs) (Wang et al., 2018) as well as activating the complement pathway (Vidarsson et al., 2014). For example, autoantibody against aquaporin-4 (AQP4) in Neuromyelitis optica (NMO) has been reported to bind not only to AQP4 on astrocytes, but also engage astrocytic Fc gamma receptors (Fc $\gamma$ Rs), via their Fc region, leading to clustering and internalization of AQP4 from the surface of astrocytes (Hinson et al., 2017). Bound AQP4 reactive autoantibody also activates C1q, due to their Fc-Fc region interaction, providing a scaffold for complement deposition, which leads to complement-dependent cytotoxicity (CDC) (Soltys et al., 2019). In another study, therapeutic antibodies targeting tau, thereby blocking its cell to cell spreading, were found to engage Fc $\gamma$ Rs on microglia promoting inflammation and the secretion of pro-inflammatory cytokines contributing to poor neuronal health (Lee et al., 2016).

Microglia are resident immune cells, of monocytic lineage, of the central nervous system (CNS) (Saijo & Glass, 2011). Within the CNS, microglia perform several important functions including synaptic pruning during development (Schafer et al., 2012) and degenerative disorders like Alzheimer's Disease (Hong et al., 2016). They also produce pro-inflammatory and anti-inflammatory cytokines and chemokines such as IL6, TNF- $\alpha$  (Smith et al., 2012) and IL10, IL4 (Pozzo et al., 2019), respectively. They are also actively engaged in the phagocytosis of cellular debris, arising from damaged neurons, via phagocytic receptors such as Toll-like receptors (TLRs), Fc $\gamma$ Rs and complement receptors, among others (Fu et al., 2014). Studies on post-mortem tissues from patients with NMDAR encephalitis have shown marked microglia activation and microgliosis in the hippocampus (Camdessanché et al., 2011; Josep Dalmau et al., 2007; Tüzün et al., 2009). Recent studies on maternal transfer of autoantibodies have also hinted at the role of microglia in autoimmune encephalitis. For example, the gestational transfer of Contactin-associated protein-like2 (CASPR2) autoantibodies induced long-term microglial activation related to synaptic loss and behavioral deficits (Coutinho et al., 2017). Similarly, brains from fetuses with placental transfer of NMDAR reactive autoantibodies showed decreased NMDAR clusters, reduced synapse number, poor behavioral performance and microglia activation (García-Serra et al., 2021). However, the casual link between the autoantibody-induced phenotypes and microglial activation remains unexplored.

Here, we investigated the capacity of patient-derived monoclonal NR1 reactive autoantibody (hNR1-mAb) to elicit a downstream immune reaction, by engaging microglia, in a neuron: microglia co-culture system. Our data revealed that microglia not only proactively remove hNR1-mAb bound NMDARs complexes, but also excitatory post-synaptic proteins in a highly specific and selective manner. Furthermore, we could show that by introducing mutations in the Fc region that blocks Fc region-driven microglia engagement prevented the loss of NMDARs and post-synaptic proteins. Similarly, utilizing patient-derived monoclonal autoantibody targeting  $\alpha$ 1 subunit of the GABA $_A$  receptor ( $\alpha$ 1-GABA $_A$ R-mAb), we could also show that microglia selectively removes autoantibody-bound GABA $_A$ Rs, but not antibody-free NMDARs and vice versa. These results provide evidence that microglia could play an active role in removing

antibody/receptor complexes, contributing to disease progression, in patients with autoimmune encephalitis.

## 2 | MATERIALS AND METHODS

### 2.1 | Preparation of hippocampal neurons

Wild type (WT) hippocampal neurons from both sexes of C57BL/6J mouse pups were plated on glass coverslips (VWR, 18 mm) supported with wax spacer dots over a bed of astrocytes, using a Banker protocol (Banker & Goslin, 1988; Meberg & Miller, 2003). In brief, astrocytes from WT cortices (P0-P2) were plated on 12 well plates at a density of 10,000 cells per 1 cm<sup>2</sup> 6–7 days in Dulbecco's Modified Eagle's Medium (DMEM, Invitrogen, Thermo Fisher Scientific) with 10% FBS, 5% PenStrep (Thermo Fisher Scientific). Astrocytes were treated with 1% floxuridine (FUDR) at 4 days *in-vitro* (DIV) to stop mitogenesis prior to addition of neurons. The medium of the astrocytes is changed to Neurobasal-A (NBA) medium with 2% B27, 1% Glutamax, 0.2% PenStrep (Thermo Fisher Scientific) at 7 DIV prior to addition of neurons. Hippocampal neurons were dissected from WT P0-P2 pups in cold Hanks' Balanced Salt solution (HBSS, Millipore). The dissected hippocampus was incubated for 30 min in enzyme solution DMEM with 3.3 mM Cystein, 2 mM CaCl<sub>2</sub>, 1 mM EDTA and 20 U/ml Papain (Worthington) at 37°C. Papain activity was inhibited by incubating hippocampus in inhibitory solution, DMEM with 10% FCS (Thermo Fisher Scientific), 38 mM BSA (Sigma-Aldrich) and 95 mM trypsin inhibitor (Sigma-Aldrich) for 5 min. Cells were titrated in NBA medium with 2% B27, 1% Glutamax, and 0.2% PenStrep by gently pipetting. Isolated neurons were then plated at a density of 20,000 cells per 1 cm<sup>2</sup> on nitric acid washed, poly-L-lysine coated glass coverslips with paraffin wax spacer dots at the bottom in NBA medium with 2% B27, 1% Glutamax, 0.2% P/S. Coverslips were transferred, with neurons facing upwards, 1.5 h later on to the wells with astrocytes in NBA medium with 2% B27, 1% Glutamax, 0.2% P/S. The neurons were cultured with astrocytes for 15–17 DIV before each experiment.

### 2.2 | Mixed glial cultures

WT cortices from P0-P2 pups were used to prepare mixed glial cultures, that is, astrocytes and microglia. The cortices were incubated with 0.05% Trypsin-EDTA (Gibco) at 37°C shaking at 800 rpm for 20 min. The trypsin was subsequently blocked with pre-warmed DMEM with 10% FBS, 5% PenStrep at 37°C. The cells were then titrated by pipetting until the cell suspension was homogenous. The cell suspension was then added to T75 flasks containing pre-warmed DMEM with 10% FBS, 5% PenStrep at 37°C. Medium was replaced at 24 h post culturing and again at DIV 6. The cells were cultured for 15–17 DIV prior to microglia isolation.

### 2.3 | Lentivirus production

All lentiviral particles were produced at the Viral Core Facility of the Charité-Universitätsmedizin, Berlin (<https://vcf.charite.de/ed/>) as described previously (Lois et al., 2002). In brief, HEK293T cells were co-transfected with 10 µg of shuttle vector, 5 µg of helper plasmid pCMVsR8.9 and 5 µg pf pVSV.G with X-tremeGENE 9 DNA transfection reagent (Roche Diagnostics). Cell culture supernatant containing the viral particles was collected 72 h post transfection and purified via filtration. Aliquots were flash frozen in liquid nitrogen and stored at –80°C. WT hippocampal neurons were infected with 100 µL per well of lentivirus at 3–4 DIV.

### 2.4 | Isolation and production of recombinant monoclonal antibody

A human IgG1 autoantibody reactive to the NR1 subunit of NMDAR (#003-102) was isolated and cloned from the CSF of patient-derived B-cells with acute NMDAR encephalitis (Kreye et al., 2016). The NR1 #003-102 was recombinantly expressed using paired expression vectors encoding for heavy and light chain by transient transfection in HEK293 cell. Following expression, the recombinant NR1 reactive autoantibody (hNR1-mAb) was purified from the supernatant as described previously (Kreye et al., 2016). The hNR1-mAb concentration was determined using anti-human IgG ELISA following the manufacturer's instructions (3850-1AD-6, Mabtech). An IgG1 autoantibody against the  $\alpha$ 1 subunit of the GABA<sub>A</sub>R ( $\alpha$ 1-GABA<sub>A</sub>R-mAb) (Kreye et al., 2021) was also isolated, cloned, expressed and purified, as mentioned above.

### 2.5 | Mutant hNR1-mAb cloning and purification

Several mutations within the Fc region of human IgG1 antibodies have been shown to block its interaction with complement proteins and FcγR. Some of these were identified to block either both of these interactions-, (Leu234Ala/Leu235Ala/Pro329Gly (LALA-PG)) or selectively complement (Pro329Ala (PA)) or FcγR binding (Leu234Ala/Leu235Ala (LALA)) (Lo et al., 2017; Saunders, 2019). Recombinant heavy chain constant region DNA segments, containing these mutations were designed and synthesized (EurofinsGenomics). The fragments were then PCR amplified with 5'-CTCAGCGTCGACCAAGGGAC-CATCGGTCTTC-3' (Forward Primer) and 5'-CATGAGCGTACGT-CATTGCCGGGGCTCAGG-3' (Reverse Primer), introducing Sall and BsiWI restriction sites at the front and back of the inserts, respectively, before subcloning into the Sall and BsiWI sites in the pCMV-hNR1-mAb (Kreye et al., 2016) vector using Quick Ligation kit (NEB, M2200). This led to the generation of expression vectors coding WT, LALA-PG, PA and LALA hNR1-mAb, respectively. Antibodies were then produced and purified from these expression vectors by new/Era/mabs GmbH, Potsdam, DE.

## 2.6 | Mouse FcγR1 and C1q binding ELISAs

WT and mutant hNR1-mAb binding to FcγR1 and C1q were measured as reported previously (Lo et al., 2017). In brief: for FcγR1 binding, purified FcγR1 protein (Sino Biological, 50086-M08H) was coated at a concentration of 1 µg/mL in PBS overnight at 4°C on 96 well plates (Corning, Costar, 3595). These were washed with PBS containing 0.05% Tween 20 (PBS-T) followed by blocking with PBS containing 0.5% BSA, 15 ppm Proclin (Sigma Aldrich, 49376-U), pH 7.4 for 1 h at room temperature (RT). Plates were further washed with PBS-T. WT and mutant (LALA-PG, PA and LALA) hNR1-mAbs (50–0.2 µg/mL in triplicates) in PBS-T containing 0.5% BSA and 15 ppm Proclin, pH 7.4, were added to the plates and incubated at RT for 2 h. Plates were washed with PBS-T and then incubated with goat F(ab')<sub>2</sub> anti-human F(ab')<sub>2</sub> conjugated with Horseradish Peroxidase (HRSP) (1:5000) (Jackson ImmunoResearch, 109-035-006) for 90 min at RT. Plates were washed with PBS-T and bound autoantibody was detected by using 3,3',5,5'-teramethylbenzidine (TMB) as a substrate (Sera Care, 5120-0047). Plates were developed with TMB in the dark at RT for 1 h. The reaction was stopped by the addition of 1 M H<sub>3</sub>PO<sub>4</sub> (Sigma Aldrich, 345245). The absorbance was then measure at 450 nm, using absorbance at 620 nm as background, using an Infinite 200PRO Tecan plate reader. The absorbance curves were subsequently plotted using GraphPad.

For mouse C1q binding, 96 well plates (Corning, Costar, 3595) were coated overnight with WT and mutant (LALA-PG, LALA and PA) hNR1-mAbs (0.1–10 µg/mL) in PBS at 4°C. Plates were then washed with PBS-T and blocked with PBS-T containing 0.5% BSA, 15 ppm Proclin and 10% blocker Caesin (ThermoFisher Scientific, 37582) (pH 7.4) for 1 h at RT. Purified mouse C1q (Complement Technology, M099) was added to the plate at a concentration of 0.5 µg/mL in PBS-T and incubated 1.5 h at RT. Plates were washed with PBS-T and bound C1q was detected by addition of biotinylated anti mouse C1q (Hycult Technologies, HM1096BT-50UG) at a concentration of 20 ng/mL for 1.5 h at RT followed by an incubation with HRSP-conjugated Streptavidin (Cytiva, RPN 1231) at a ratio of 1:5000 for 1 h at RT. Plates were washed with PBS-T and developed using TMB substrate for 1 h in the dark. The reaction was subsequently stopped using 1 M H<sub>3</sub>PO<sub>4</sub>. The absorbance was then measured at 450 and 620 nm, using Infinite 200PRO Tecan plate reader, which automatically subtracts the background signal at 620 nm. The absorbance curves were subsequently plotted using GraphPad. Note, washing was always done at least three times with PBS-T while maintaining reaction volume at 100 µL per well. Gentle shaking (50 rpm) was performed during each incubation step.

## 2.7 | Pre-labeling of hNR1-mAb

hNR1-mAb autoantibody, 1 µg per coverslip, was pre-labeled using Zenon Human IgG Labeling Kit (Molecular Probes, Z-25408, Z-25407 or Z-25402), following the manufacturer's protocol. Briefly, 1 µg of hNR1-mAb in PBS was incubated with 5 µL of labeling Reagent A

(200 µg Fab fragment/ml, 5 mM azide) followed by 5 min incubation at RT. Five microliters of blocking Reagent B (5 mg IgG/ml, 5 mM azide) was then added to the solution and incubated at RT for 5 min. Note, pre-labeling involves attachment of Fab fragments tagged to fluorophores at the Fc region of the antibody, which could interfere with binding to complement proteins and/or FcγRs. Thus, cells were incubated with a 1:1 mixture of pre-labeled and unlabeled autoantibody. Previous studies have used different concentration of hNR1 autoantibody *in-vitro* like 0.5 µg/mL (Kreye et al., 2016) or 1 µg/mL (Andrzejak et al., 2022) without washing out for 24 h. Here, a final concentration of 2 µg/mL of the autoantibody (pre- and unlabeled at 1 µg/mL each) was added to co-culture set up as this amount was found to optimally label NMDARs within the acute time frame of 30 min. Such an amount was found to be sufficient to saturation binding, while 95% of added hNR1-mAb was washed off after 30 min.

## 2.8 | Neuron microglia co-culture

### 2.8.1 | Bound hNR1-mAb removal experiment

Cultured hippocampal neurons were incubated with hNR1-mAb at DIV 15–17. Here, 1 µg of the pre-labeled (hNR1-mAb\*) and unlabeled (hNR1-mAb) hNR1-mAb mixture (1:1) was added to the coverslips making the final concentration 2 µg/mL. hNR1-mAb\*/hNR1-mAb were allowed to bind to the neurons for 30 min at 37°C. Medium with unbound autoantibodies were then removed and replenished with fresh pre-warmed NBA medium with 2% B27, 1% Glutamax, and 0.2% PenStrep.

Primary mouse microglia, grown for 15–17 DIV, were isolated by tapping mixed glial flasks manually for 6 min. The supernatant containing microglia was centrifuged at 200g at 22°C for 5 min. The cell pellet was resuspended in pre-warmed NBA medium at 37°C with 2% B27, 1% Glutamax, 0.2% P/S. Cell number was counted using hemocytometer. Microglia cells were added to the autoantibody-bound neurons at a density, ensuring a 1:3 microglia:neuron ratio. Different ratios of microglia to neuron, 1:2, 1:3 and 1:5, were also tested, yet 1:3 microglia to neuron ratio was found to be optimal in both cellular health and density of both cell types and thus used for all subsequent experiments. Microglial cells were incubated with autoantibody-bound neurons for 1, 3 and 6 h at 37°C following which the cells were fixed with pre-warmed 4% paraformaldehyde (PFA) for 10 min, prior to immunocytochemical staining (see below).

### 2.8.2 | NMDAR/hNR1-mAb complex removal experiment

For studying microglia-mediated removal of NMDAR/hNR1-mAb complexes, WT hippocampal neurons were initially infected with 200 µL per well of lentiviruses expressing NR1-EGFP under the neuron specific Synapsin promoter at 3–4 DIV, and subsequently incubated with hNR1-mAb\*/hNR1-mAb (2 µg/mL) at 37°C for 30 min at



(15–17 DIV). After incubation and removal of unbound autoantibody, microglia were added to the neurons in 1:3 ratio of microglia to neuron for 6 h at 37°C. Cells were then fixed with pre-warmed 4% PFA for 10 min. Cells were stained with anti-GFP (1:1000, mouse, Abcam, #ab1218) antibody to enhance NR1-EGFP signal.

### 2.8.3 | Synapse quantification experiment

WT hippocampal neurons (DIV 15–17) were treated with unlabeled hNR1-mAb for 30 min at 37°C. Directly after unbound hNR1-mAb removal, microglia were added to autoantibody-bound neurons for 6 h as described above. Cells were fixed with pre-warmed 4% PFA and later stained for the post-synaptic and pre-synaptic marker proteins, PSD95 and vGLUT1, respectively.

To directly monitor the loss of synapses in presence of microglia, in some experiments WT hippocampal neurons were doubly infected with lentiviruses expressing either mCh-Synapsin/Homer-EGFP (Homer-1) or Synaptophysin-EGFP/PSD95-mKate2 on DIV 3–4 under the neuron specific Synapsin promoter. Neurons overexpressing different combinations of pre- and post-synaptic markers were then treated with unlabeled hNR1-mAb (2 µg/mL) for 30 min at 37°C, before washing and adding microglia for 6 h as described above. Finally, the cells were fixed in 4% PFA and subsequently processed for immunocytochemistry.

### 2.8.4 | Mutant hNR1-mAb experiments

As described above for experiments with WT hNR1-mAb\*/hNR1-mAb, we also treated WT hippocampal neurons with LALA-PG or LALA or PA mutants of hNR1-mAb prepared in a 1:1 mixture of pre-labeled:unlabeled autoantibodies. Following the removal of unbound antibodies by washing, microglia were added for 6 h at 37°C. Cells were then fixed with pre-warmed 4% PFA for 10 min.

### 2.8.5 | Antibody specificity experiments

To study the specificity of microglia-mediated removal of bound autoantibody, we compared the ability of microglia to remove the hNR1-mAb\*/hNR1-mAb to that of a second patient-derived autoantibody against the alpha1 subunit of the GABA<sub>A</sub>R (α1-GABA<sub>A</sub>R-mAb). Here, pre-labeling of α1-GABA<sub>A</sub>R-mAb (GABA<sub>A</sub>R-mAb\*) was performed as mentioned before, however in this case 8.3 µL of Reagent A and Reagent B of Zenon kit (Alexa 647, Molecular Probes, Z-25408) was used as the labeling was not uniform for lower antibody to reagent ratios. Initially, we checked if bound α1-GABA<sub>A</sub>R-mAb could also trigger microglia-mediated loss of α1-GABA<sub>A</sub>R-mAb puncta similar to hNR1-mAb. This was accomplished similar to hNR1-mAb experiments in that neurons were first treated with α1-GABA<sub>A</sub>R-mAb\*/α1-GABA<sub>A</sub>R-mAb (1:1) (2 µg/mL) for 30 min followed by removal of unbound antibody and the addition of microglia for 6 h.

In co-labeling experiments, we initially incubated cultures for 30 min with α1-GABA<sub>A</sub>R-mAb\*/α1-GABA<sub>A</sub>R-mAb (1:1) (2 µg/mL) before washing and adding microglia for 6 h as described above. After 6 h, pre-labeled hNR1-mAb\* (Zenon kit Z25407, Alexa 594) (1 µg/mL) was added for 30 min to label the NMDARs. Cells were then washed with pre-warmed NBA culture medium before fixation with 4% PFA. The converse experiment was performed by first adding hNR1-mAb\*/hNR1-mAb (1:1) (2 µg/mL) for 30 min, washing, adding microglia for 6 h followed by incubating cultures with the α1-GABA<sub>A</sub>R-mAb\* to label GABA<sub>A</sub>Rs for 30 min.

In competitive experiments, we simultaneously added different combinations of antibodies: for example, (a) both WT GABA<sub>A</sub>R-mAb and hNR1-mAb or (b) GABA<sub>A</sub>R-mAb and LALA-PG mutant of hNR1-mAb (LALA-PGhNR1-mAb) to our co-culture setup. Here, WT hippocampal neurons were pre-treated with either hNR1-mAb\* (Alexa 647)/hNR1-mAb (1:1) and α1-GABA<sub>A</sub>R-mAb\* (Alexa 594)/α1-GABA<sub>A</sub>R-mAb (1:1) or LALA-PG-hNR1-mAb\* (Alexa 647)/LALA-PG-hNR1-mAb (1:1) and α1-GABA<sub>A</sub>R-mAb\* (Alexa 594)/α1-GABA<sub>A</sub>R-mAb (1:1) at a concentration of 2 µg/mL for each autoantibody at 37°C for 30 min. After washing of unbound antibody, microglia were added for 6 h at 37°C. Cells were then fixed with 4% PFA for 10 min.

## 2.9 | Immunocytochemistry

Cells fixed in PFA were washed two times with PBS followed by incubation with ice cold 25 mM glycine in PBS for 20 min to quench background fluorescence. Cells were then permeabilized and blocked with a solution containing 5% Normal Goat Serum (NGS), 2% BSA and 0.1% Triton in PBS for 1 h at RT. Cells were then incubated with primary antibodies in PBS containing 5% NGS and 2% BSA for 1 h at RT. The following primary antibodies were used: MAP2 (1:2000, chicken, Millipore, #AB5543), CD11b (1:1000, rat, Abcam, #ab8878), Iba1 (1:500, rabbit, Wako, #019-19741), P2Y12R (1:400, rabbit, AnaSpec, #AS-55043A), PSD95 (1:500, mouse, Abcam, #ab2723), vGLUT1 (1:4000, guinea pig, Synaptic Systems, #135 304), Lamp2a (1:1000, rabbit, Abcam, #ab18528), CD68 (1:1000, rabbit, Abcam, #ab125212) and GFP (1:1000, mouse, Abcam, #ab1218). The cells were then washed three times with PBS containing 5% NGS and 2% BSA for 10 min each. This was followed by incubation with secondary antibody diluted in PBS containing 5% NGS and 2% BSA for 1 h at RT. Differentially labeled (Alexa fluorophore) secondary antibodies (1:1000, Invitrogen, Thermo Fisher Scientific) were used. Cells were then washed three times once with PBS containing 5% NGS and 2% BSA followed by two times with cold PBS for 10 min each. Finally, coverslips were dipped in H<sub>2</sub>O and mounted on Mowiol mounting media.

## 2.10 | Electron microscopy

To study microglia-mediated removal of antibody complexes and post-synaptic proteins in the presence of bound hNR1-mAb by

electron microscopy (EM), we adapted a photo-conversion protocol that was previously described (Meisslitzer-Ruppitsch et al., 2013). This is based on the oxidation of the chromogen 3,3'-diaminobenzidine tetrahydrochloride (DAB), in presence of singlet oxygen generated by photo-bleaching, and the formation of precipitates that are electron-dense and thus can be imaged and analyzed with EM. WT hippocampal neurons were treated with pre-labeled hNR1-mAb<sup>~</sup> (Zenon kit Z25402, Alexa 488) and unlabeled hNR1-mAb in 1:1 ratio (hNR1-mAb<sup>~</sup> /hNR1-mAb) (2 µg/mL) for 30 min following which unbound antibodies were washed off. For studying removal of post-synaptic proteins, lentivirally infected neurons overexpressing Homer-EGFP under the Synapsin promoter were used, followed by addition of hNR1-mAb (2 µg/mL) for 30 min and washing away of unbound hNR1-mAb. Microglia were then added to and incubated for 90 min at 37°C. The cells were fixed in pre-warmed 1.25% glutaraldehyde (ThermoFisher) in 0.066 M sodium cacodylate buffer (Sigma Aldrich). Cells were washed three times with 0.1 M sodium cacodylate buffer for 10 min per wash. To prevent nonspecific background DAB reaction cells were blocked for 30 min at 4°C in blocking buffer (50 mM glycine and 5 mM aminotriazole in 0.1 M sodium cacodylate). This was followed by incubation with 100 mM ammonium chloride at 4°C for 1 h and washing with 0.1 M sodium cacodylate buffer. 1 mg/mL DAB (Sigma, D5905) in Tris Buffer Saline (TBS) pH 7.4 was oxygenated for 5 min at 4°C. The cells with or without bound hNR1-mAb<sup>~</sup> were then bleached using a mercury lamp (491 nm excitation laser) of Zeiss confocal microscope under 20× objective at 100% intensity for 30 min in presence of oxygenated ice cold 1 mg/mL DAB in TBS. The cells were then washed with chilled 0.1 M sodium cacodylate followed by 1 h incubation with 1% osmium tetroxide (Science Services) in 0.1 M sodium cacodylate. After this, cells were en-bloc stained and embedded in Epoxy resin (Epon 812 Kit, Science Services) following steps 3–15 of this protocol <https://www.protocols.io/view/chemical-fixation-and-embedding-of-cultured-cells-eq2lyp5yplx9/v1>. The photo-converted area from each experimental group was visible due to the formation of a brown precipitate. The photo-converted region was subsequently cut with a Ultracut ultramicrotome (Leica) equipped with a 45° Ultra diamond knife (Diatom). Sixty nanometers thick ultrathin sections were collected on formvar coated copper grids (Science Services) stained for 5 min with 1% uranyl acetate and for 1 min with 1% lead citrate and imaged at an EM900 Transmission Electron Microscope (Zeiss) operating at 80 kV and equipped with a 2k × 2k digital camera (Olympus). To note, either Alexa 488 pre-labeled hNR1-mAb<sup>~</sup> or Homer-EGFP was used as fluorophores of choice for photo-conversion as they have the highest yield of reactive oxygen species (ROS) upon bleaching which ensures efficient DAB precipitation.

## 2.11 | Live imaging

For live imaging of microglia-mediated removal of NMDAR/hNR1-mAb complexes, WT hippocampal neurons infected with lentiviruses expressing NR1-EGFP at 3 DIV were treated with pre-labeled/

unlabeled hNR1-mAb<sup>~</sup>/hNR1-mAb (1:1) (2 µg/mL) for 30 min at 37°C at 15–17 DIV. After washing away unbound antibody, microglia were added to the neurons for 1 h. The coverslips with hNR1-mAb bound neurons and microglia were then carefully transferred to a live imaging chamber (Quick Change Chamber for 18 mm, RC-41LP, Warner Instruments) together with 500 µL of NBA culture media. Coverslips were then imaged using a Nikon Spinning Disk Confocal Microscope (AMBIO Facility, Charité-Universitätsmedizin, Berlin) under 40× water objective. Six different regions with neuron and microglia were selected and the focus and Z plane of each of these regions were defined. Images were taken using DualCamera set up of the microscope with one camera for taking differential interference contrast (DIC) images while the other collected fluorescence images. The cells were imaged live at 37°C for 1 h under perfect focus setting of the confocal microscope with no wait time. Note, after the sixth image the microscope immediately returns to the first region of interest (ROI). The images were processed with volume projection in time series using Imaris 9.0.0 software.

## 2.12 | Image acquisition and quantification

Fluorescent images were acquired on either a spinning disk confocal microscope (Carl Zeiss Axio Observer.Z1 with Andor spinning disk and cobolt, omnicon, i-beam laser) (Carl Zeiss, Andor) using a 40× (1.3 NA) Plan-Apochromat oil objective and an iXon ultra (Andor) camera controlled by iQ software (Andor) or a Nikon Spinning Disk Confocal under 40× (1.3 NA) objective. All images were taken with a Z stack of 5 µm with a step size of 0.5 µm. Neuronal cells of visibly similar morphology with extensive dendritic branches were imaged. Microglial cells adjacent to neuronal dendritic branches were imaged.

Images were processed and analyzed using ImageJ/FIJI software. The images were first converted into maximum intensity projections using ImageJ codes. For NMDAR and GABA<sub>A</sub>R puncta analysis, secondary dendrites (one from each quadrant per image) of around the same thickness from each experimental group were selected. ROI selection was based solely on MAP2 staining to eliminate bias. The length of the dendrite within each ROI was measured and recorded. Numbers of NMDAR/GABA<sub>A</sub>R puncta along each dendritic segment were counted using Time Series Analyzer plugin of ImageJ. Briefly, circles of 6 × 6 pixels were manually placed over NMDAR puncta along each dendrite. Puncta with intensity above a set threshold value (average intensity of least intense puncta) were counted as positive puncta. The number of puncta and intensity of each puncta was recorded using Time Series Analyzer and plotted as the number of puncta per 100 µm length of dendrite (referred henceforth as puncta/unit length).

The number of co-localizing pre- (vGLUT1 or mCh-Synapsin1 or Synaptophysin-EGFP) and post-synaptic markers (PSD95 or Homer-EGFP or PSD95-mKate2) along dendritic segments were determined as described above. In brief, synapse counting (e.g., double positive for vGLUT1+/PSD95+) was performed by placing 6 × 6 pixels circles over PSD95 positive puncta (with intensity above the set threshold

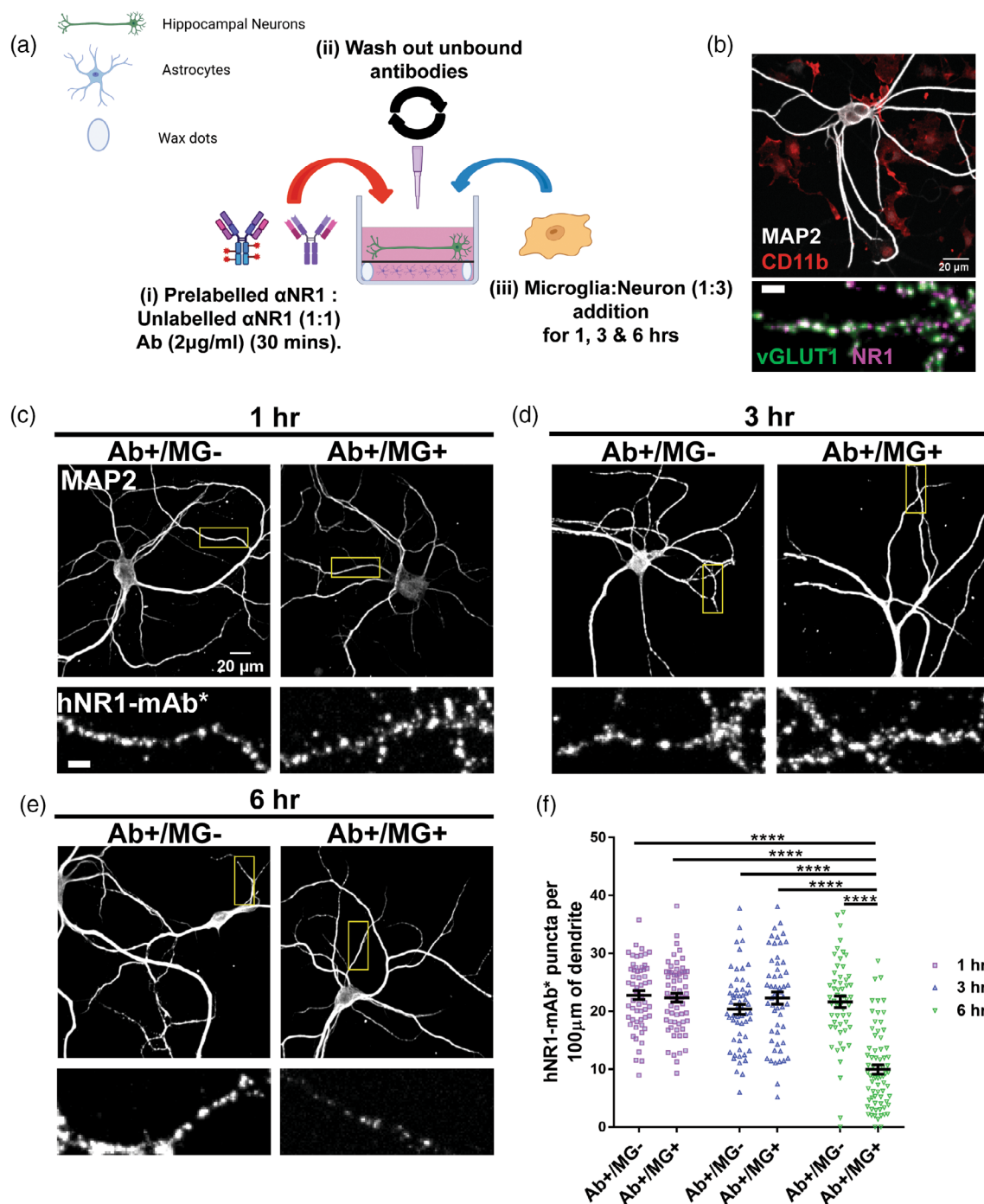


**FIGURE 1** Reduction in hNR1-mAb labeled NR1 puncta 6 h after co-culturing hNR1-mAb bound hippocampal neurons with microglia. (a) Schematic of co-culture setup of hNR1-mAb bound neuron and microglia for different time points (1, 3 and 6 h) in “Banker” like culture in which neurons are placed face up on coverslips supported by wax spacer dots over a bed of astrocytes. (b) Image of a hippocampal neuron co-cultured with microglia stained for the dendritic marker MAP2 (gray) and CD11b (red), respectively. Zoom view of dendritic segment showing synaptic co-localization (white) of bound pre-labeled hNR1-mAb\* (Alexa 647) (magenta) puncta with the pre-synaptic marker vGLUT1 (green). Scale bar, 5  $\mu\text{m}$ . (c–e) Representative images of hippocampal neurons stained for MAP2 (gray) with selected Region Of Interests (ROIs) showing bound pre-labeled hNR1-mAb\* (gray) along dendritic segments with or without microglia addition (Ab+/MG+ and Ab+/MG-, respectively) for 1, 3 and 6 h, respectively. Scale bar, 5  $\mu\text{m}$ . (f) Quantitation of hNR1-mAb\* puncta number along 100  $\mu\text{m}$  of dendrite (unit length) with and without microglia. Significant reduction in puncta number was only seen 6 h after the addition of microglia to hNR1-mAb\* bound hippocampal neurons. Each data point is an ROI from three independent experiments ( $n = 55-71$  ROIs for each group). Error bars represent standard error of mean (SEM). Two-way ANOVA with Tukey's multiple comparison test was used to evaluate statistical significance (\*\*\*\* $p < .0001$ ).

1.5× above background) along dendritic segments followed by measuring intensity of both PSD95 and vGLUT1 at these locations. The number of vGLUT1+/PSD95+ double positive synapses was then plotted per unit length of dendrite.

For analyzing uptake of different receptors and synaptic markers by microglia, microglial cells, labeled with the CD11b antibody, were selected using the Polygon selection tool of ImageJ. Then the average mean intensity of different synaptic markers within each labeled microglia area was measured. These were normalized to intensities within microglia in no autoantibody control (Ab−/MG+).

To eliminate bias, neuronal cells were selected, imaged and analyzed based solely on MAP2 staining. All ROIs after selection were numbered randomly without specifying the experimental conditions to ensure analysis was blinded.

## 2.13 | Experimental design and statistical analyses

All figures represent data from at least three independent experiments from independent cultures. Statistical design for all experiments can be found in figure legends. GraphPad Prism was used to perform all statistical tests and graphical representations. Unpaired t-tests with Welch correction, when the variances were different, was used to determine statistical significance. One way and Two-way ANOVA with Tukey's multiple comparison tests were used to compare means of different experimental groups. All data are represented as mean ± standard error of mean (SEM) with *p* values <.05 representing statistical significance. Schematics were made using [BioRender.com](https://www.biorender.com).

## 3 | RESULTS

### 3.1 | Primary mouse microglia promote the removal of hNR1-mAb labeled NR1 puncta from hippocampal neurons

To test our hypothesis that NMDAR/NR1-mAb complexes on the surface of neurons could lead to microglia engagement and receptor removal by phagocytosis, we developed an *in-vitro* co-culture system comprised of primary mouse hippocampal neuron and microglia, wherein the addition of antibodies and/or microglia could be temporally controlled (Figure 1a,b). To monitor changes in antibody/receptor distribution, we used the Zenon-system to fluorescently tag hNR1-mAb (hNR1-mAb\*, #003-102) (Kreye et al., 2016). hNR1-mAb\* along with unlabeled hNR1-mAb (hNR1-mAb/hNR1-mAb) in a ratio of 1:1 were added to live hippocampal neurons (15–17 DIV) for 30 min, allowing surface synaptic and extra-synaptic receptors to be labeled. Unbound antibodies were removed by medium exchange before addition of isolated cortical microglia at a ratio of 1:3 to neurons for various times (e.g., 1–6 h). In neuronal cultures, lacking microglia, the fluorescently labeled hNR1-mAb\* puncta readily decorated

the surfaces of MAP2 positive dendrites in pattern that co-localized with the pre-synaptic glutamatergic synaptic vesicle marker vGLUT1 (Figure 1b), consistent with the post-synaptic localization of NMDARs and this antibody, as previously described (Kreye et al., 2016). In cultures that also received microglia for 1, 3 or 6 h, we observed a qualitative decrease in the number of hNR1-mAb\* positive puncta along dendrites over time (Figure 1c–e). Quantifying the number of puncta/unit length of dendrite at 1, 3 and 6 h after microglia addition, revealed a significant decrease in the number of hNR1-mAb\* positive puncta 6 h after the addition of microglia to the hippocampal neuronal cultures ( $22.34 \pm 0.761$ ,  $22.31 \pm 1.006$  and  $9.964 \pm 0.8024$  of Ab+/MG+ for 1, 3 and 6 h, respectively,  $p < .0001$ ) (Figure 1e,f). No significant decrease in the number of hNR1-mAb\* positive puncta/unit length of dendrite was detected either at 1 h (Figure 1c,f) or 3 h (Figure 1d,f) post microglia addition. Importantly, no change in the number of NR1-mAb\* positive puncta was observed in the absence of microglia for 1, 3 or 6 h ( $22.79 \pm 0.7698$ ,  $20.35 \pm 0.8721$  and  $21.63 \pm 0.9782$  of Ab+/MG− for 1, 3 and 6 h, respectively) (Figure 1f), indicating that antibody-mediated receptor internalization does not play significant role in removal of bound receptors in this time frame, consistent with previous studies (van Casteren et al., 2022). Note, several studies have reported that the internalization driven the loss of NMDARs and NMDA currents in presence of hNR1 autoantibody at longer time points, that is, 12–24 h (Andrzejak et al., 2022; Jézéquel et al., 2017; Moscato et al., 2014). To explore the effect of microglia-mediated removal of bound hNR1-mAb at longer time scales, we performed the co-culture experiment for 6 and 24 h with or without microglia addition. Here, we found a similar significant decrease in the number of hNR1-mAb\* puncta along dendrite 6 h after microglia addition (Figure S1a,b). Interestingly, an almost significant decrease ( $p = .056$ ) in hNR1-mAb\* puncta number was seen after 24 h even without microglia addition which could be due to previously reported internalization of NMDARs bound with hNR1-mAb. However, microglia addition led to a further decrease in hNR1-mAb\* after 24 h (Figure S1a,b). Hence, to reduce the contribution of internalization-driven effects, all subsequent co-culture experiments were performed for 6 h.

### 3.2 | Bound hNR1-mAb is removed by microglia and accumulates in microglial endo-lysosomes

To investigate whether microglia physically removed the bound hNR1 autoantibody, we analyzed whether the hNR1-mAb\* accumulated in the soma of microglia, following the 1, 3 or 6 h incubation with hNR1-mAb\*/hNR1-mAb bound hippocampal neurons. In cultures fixed and stained with antibodies against CD11b, a microglia marker, clear hNR1-mAb\* positive puncta could be detected within CD11b positive microglia at significantly higher levels 3 and 6 h (Figure 2a,b) after co-culturing with NR1-mAb bound hippocampal neurons. These increases were not associated with appreciable changes in the fluorescent intensity of CD11b in these hNR1-mAb\* positive microglial



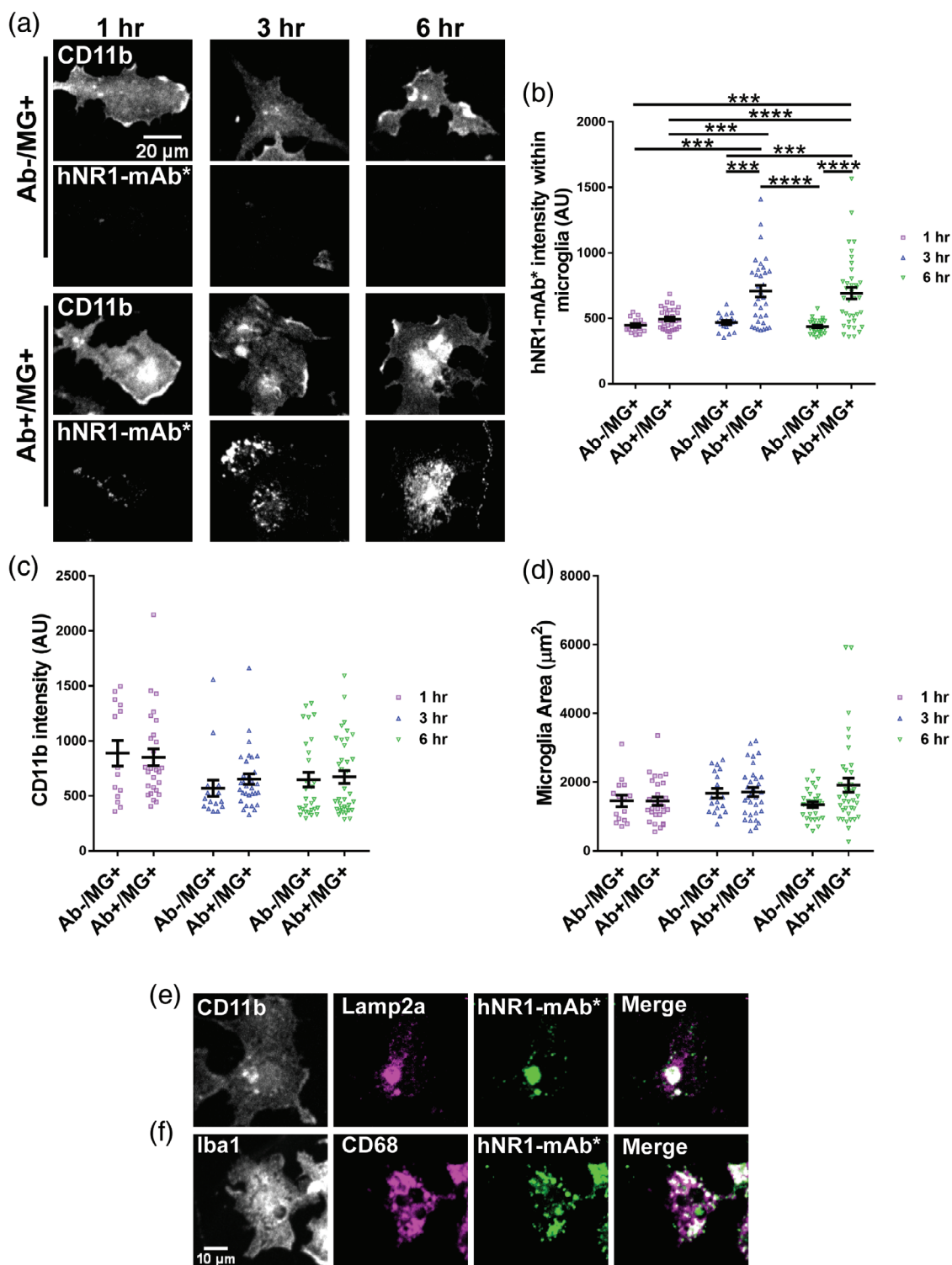


**FIGURE 2** NMDAR immuno-reactivity accumulates within microglial endo-lysosomes. (a) Images of microglia, stained for CD11b (gray), 1, 3 and 6 h after co-culture with neurons with or without hNR1-mAb\* (Ab+/MG+ and Ab-/MG+, respectively). hNR1-mAb\* (gray) puncta accumulate in microglia when co-cultured with hNR1-mAb\* bound neurons (Ab+/MG+). (b) Increased hNR1-mAb\* immunoreactivity inside CD11b positive microglia after 3 and 6 h of co-culture with neurons in presence of hNR1-mAb\*. Each data point represents one microglial cell from three independent experiments ( $n = 20$ –37 cells for each group). Error bars represent standard error of mean (SEM). Two-way ANOVA with Tukey's multiple comparison test was used to evaluate statistical significance ( $***p < .0002$ ;  $****p < .0001$ ). (c and d) CD11b intensity and microglia area, respectively, remained unchanged 1, 3 and 6 h after co-culture with or without bound hNR1-mAb\*. Each data point represents one microglial cell from three independent experiments ( $n = 20$ –37 cells for each group). Error bars represent SEM. Two-way ANOVA with Tukey's multiple comparison test was used to evaluate statistical significance. (e and f) hNR1-mAb\* puncta (green) inside CD11b or Iba-1 positive microglia cell (gray) co-localized with a pan lysosomal marker, Lamp2a or monocytic lysosomal marker, CD68 (magenta), respectively.



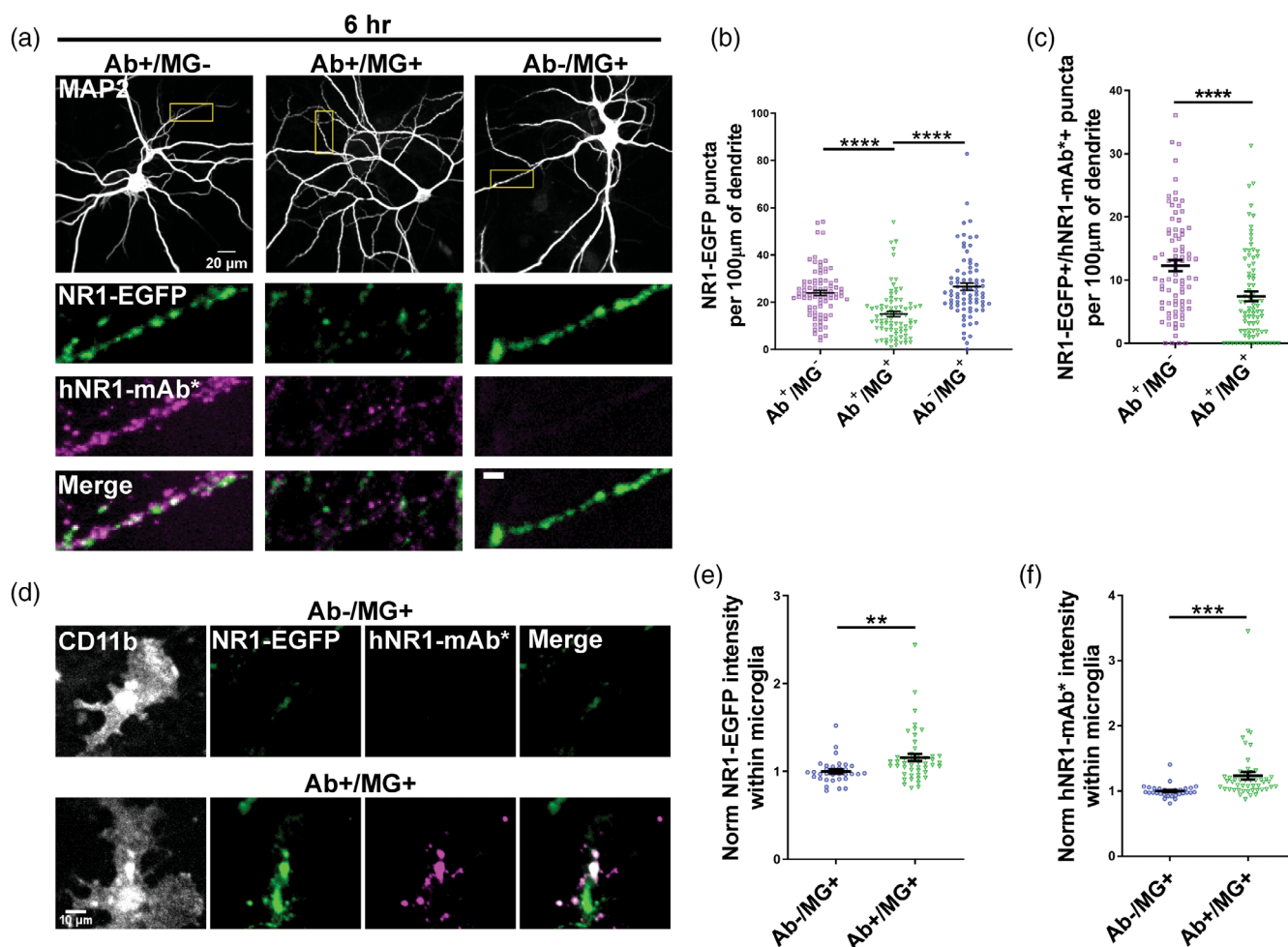


**FIGURE 3** hNR1-mAb induces microglial-dependent removal of NR1-EGFP from hippocampal neurons. (a) Representative images of neurons overexpressing NR1-EGFP co-cultured with microglia for 6 h with or without bound pre-labeled hNR1-mAb\* (Ab+/MG+ and Ab-/MG+, respectively) and stained for MAP2 (gray). Ab+/MG- experimental group without microglia addition to hNR1-mAb\* bound NR1-EGFP overexpressing neurons was also included. Selected ROIs shows NR1-EGFP (green), hNR1-mAb\* (magenta) and their merge (white) puncta along dendritic segments (scale bar, 5 μm). (b) Quantitation of NR1-EGFP puncta number per unit length of dendrite. There is a significant reduction of NR1-EGFP puncta number only in presence of microglia and hNR1-mAb (Ab+/MG+) after 6 h of co-culture. Each data point represents an ROI from three independent experiments ( $n = 82$  for Ab+/MG-,  $n = 82$  for Ab+/MG+ and  $n = 78$  for Ab-/MG+). Error bars represent SEM. One-way ANOVA with Tukey's multiple comparison test was used to evaluate statistical significance (\*\*\*\* $p < .0001$ ). (c) Quantification of NR1-EGFP/hNR1-mAb\* double positive puncta along dendrites. A significant reduction was seen in Ab+/MG+ compared to Ab-/MG+ group after 6 h. Each data point represents an ROI from three independent experiments ( $n = 78$  for Ab-/MG+ and  $n = 82$  for Ab+/MG+). Unpaired  $t$ -test was used to evaluate statistical significance (\*\*\*\* $p < .0001$ ). (d) Images of CD11b positive microglia cells (gray), revealing immunoreactivity for both NR1-EGFP (green) and hNR1-mAb\* (magenta) in the Ab+/MG+ group after 6 h of co-culture. Such NR1-EGFP (green) and hNR1-mAb\* (magenta) puncta were not seen inside microglia in absence of hNR1-mAb (Ab-/MG+). (e and f) Normalized intensity of NR1-EGFP and hNR1-mAb\* inside microglia was significantly higher in Ab+/MG+ compared to the Ab-/MG+ group. Each data point represents a microglia cell over three independent experiments ( $n = 32$  for Ab-/MG+ and  $n = 48$  for Ab+/MG+). Error bars represent SEM. Unpaired  $t$ -test with Welch correction was used to evaluate statistical significance (\*\* $p = .0019$  \*\*\* $p = .0003$ ).

(Figure 2a,c). To assess whether the addition of antibodies affects the activation state of added microglia, we monitored the *in-vitro* expression of several other physiologically relevant microglial markers, including Iba1 and P2Y12R, which have previously also been used to determine the activation state of microglia (Hovens et al., 2014; Walker et al., 2020). Microglial cells used in our co-culture experiments were found to express both Iba1 and P2Y12R with no appreciable changes in morphology (Figure S2a). Moreover, we also found

that the expression levels of both Iba1 and P2Y12R did not change significantly 1 and 6 h after co-culture (Figure S2b-d). These data could imply that our co-culture conditions do not led to significant microglia activation.

Typically, antibody/receptor complexes phagocytosed by microglia are subsequently degraded via the endo-lysosomal system. To explore this possibility, microglia were immuno-stained 6 h after co-culture with antibodies against Lamp2a, a lysosomal-associated

membrane protein or CD68, an endo-lysosomal associated membrane protein in cells of the monocytic lineage. Here, hNR1-mAb\* positive puncta were found to co-localize with Lamp2a or CD68 positive endo-lysosomes within CD11b or Iba1 positive microglia, respectively (Figure 2e,f), consistent with their clearance via this degradative system.

To further validate the observation that microglia remove and internalize bound hNR1-mAb from the surface of neurons, we performed EM following DAB incubation and Alexa 488 photo conversion 90 min after microglia addition to hippocampal neurons bound with pre-labeled hNR1-mAb<sup>~</sup> (Zenon Kit Z25402, Alexa 488) and unlabeled hNR1-mAb, hNR1-mAb/hNR1-mAb<sup>~</sup> (1:1). EM images of microglia revealed the presence of electron-dense material inside membrane bound structures within microglia in the Ab+/MG+ condition (Figure S3b). This was rarely detectable in cultures lacking the hNR1-mAb, that is, Ab-/MG+ condition (Figure S3a). Instead, in the latter, we observed electron-dense signal restricted to mitochondria, due to the photo-conversion of reactive oxygen species that are generated during the mitochondrial ATP generation process (Figure S3a, b). These data support our immunocytochemistry results showing that bound hNR1-mAb can be removed from the surface of neurons by microglia (Figure 2).

### 3.3 | Microglia removes NMDAR/hNR1-mAb complexes from the surface of neurons

Given our experimental design, namely that unbound antibody is washed away following a 30 min incubation, we anticipated that the appearance of hNR1-mAb\* within microglia is associated with and involved in the co-removal of antibody/NMDAR complexes by microglia. To formally test this hypothesis, we infected mouse hippocampal neuron with a lentivirus expressing NR1-EGFP under the neuron specific Synapsin promoter at DIV 3. At 15–16 DIV, these cultures were initially incubated with hNR1-mAb\*/hNR1-mAb for 30 min, washed to remove unbound antibody and incubated with microglia for 6 h. This led to a significant decrease in the number of NR1-EGFP puncta per unit length of dendrite in the presence of microglia ( $23.96 \pm 1.148$  for Ab+/MG– vs.  $15.01 \pm 1.164$  for Ab+/MG+,  $p < .0001$ ) (Figure 3a,b). Moreover, this decrease was associated with a decline in the number of NR1-mAb\* and NR1-EGFP double positive puncta after 6 h of co-culture ( $12.28 \pm 0.8791$  for Ab+/MG– vs.  $7.424 \pm 0.7787$  for Ab+/MG+,  $p < .0001$ ) (Figure 3c). No decrease in NR1-EGFP puncta number was detected after 6 h of co-culture with microglia in the absence of bound hNR1-mAb\* ( $23.96 \pm 1.148$  for Ab+/MG– vs.  $26.64 \pm 1.573$  for Ab-/MG+,  $p = .3170$ ) (Figure 3a,b). Importantly, we also observed a concomitant increase in the fluorescent intensity of NR1-EGFP and hNR1-mAb\* double positive puncta inside microglial cells (Figure 3d–f).

To complement these experiments, we also performed live experiments to monitor the real-time removal of NR1-EGFP decorated with

hNR1-mAb\*/hNR1-mAb by microglia. Using differential interference contrast (DIC) and fluorescence imaging, we could simultaneously visualize neuronal networks and microglia in addition to NR1-EGFP and hNR1-mAb\* fluorescence (Figure 4a). Live imaging 1 h after the addition of microglia revealed the active uptake of double positive hNR1-mAb\* and NR1-EGFP puncta by microglia from dendritic branches (Figure 4b) (Figure S4a,b). In some cases, we could visualize long microglial processes removing NR1-EGFP/hNR1-mAb\* puncta and the pulling of these complexes toward its cell body from dendritic arbors (Figure S4c). Notably, a greater accumulation of hNR1-mAb\* was observed inside microglia as compared to NR1-EGFP (Figure 4b). This could be due to the low/moderate expression of NR1-EGFP following transfection, compared to the higher levels of NMDAR-bound hNR1-mAb\* to these neurons. Moreover, it is well appreciated that EGFP is more effectively quenched inside acidic lysosomes compared to Alexa 647, used in the pre-labeling of hNR1-mAb\* (A. K. Chen et al., 2008). Together these data indicate that microglia can indeed actively remove NMDAR/hNR1-mAb complexes within 1 h of their initial engagement.

### 3.4 | hNR1-mAb promotes microglia-mediated synapse loss

Intrauterine exposure to IgG1 from anti-NMDAR encephalitis patient was recently shown to cause synapse loss and microglia activation in the brains of postnatal mice (García-Serra et al., 2021). This raises a fundamental question of whether synapse loss is secondary to the removal of antibody/NMDARs complexes and/or whether microglia encounter these complexes and simultaneously remove/strip away excitatory synapses. As an initial test of this concept, we co-cultured hNR1-mAb\*/hNR1-mAb bound hippocampal neuron with microglia for 6 h and then analyzed changes in the number of synapses, defined as puncta double positive for the excitatory pre-/post-synaptic markers, vGLUT1 and PSD95, respectively (Figure 5a). Here, we observed a significant decrease (~20%) in the number of vGLUT1+/PSD95+ double positive puncta/unit length of dendrite in the presence of autoantibody and microglia after 6 h ( $18.87 \pm 0.9258$  for Ab+/MG– vs.  $14.19 \pm 0.7152$  for Ab+/MG+,  $p = .0005$ ) (Figure 5b). Interestingly, a similar decrease was observed only in the number of PSD95 positive puncta ( $22.03 \pm 0.7569$  for Ab+/MG– vs.  $15.8 \pm 0.7200$  for Ab+/MG+,  $p < .0001$ ) (Figure 5c), but not in the number of vGLUT1 positive puncta/unit length of dendrite ( $22.57 \pm 0.9887$  for Ab+/MG– vs.  $21.89 \pm 0.9218$  for Ab+/MG+,  $p = .9586$ ) (Figure 5d), suggesting that microglia preferential remove the post-synaptic components of excitatory synapses. Importantly, no decrease was observed in any of the other experimental conditions, that is, untreated, no microglia (Ab+/MG–) or no NR1 autoantibody (Ab-/MG+). To assess whether these changes were due to their engulfment by microglia, we also analyzed whether either protein accumulated in microglia after 6 h of co-culture. Similar to results



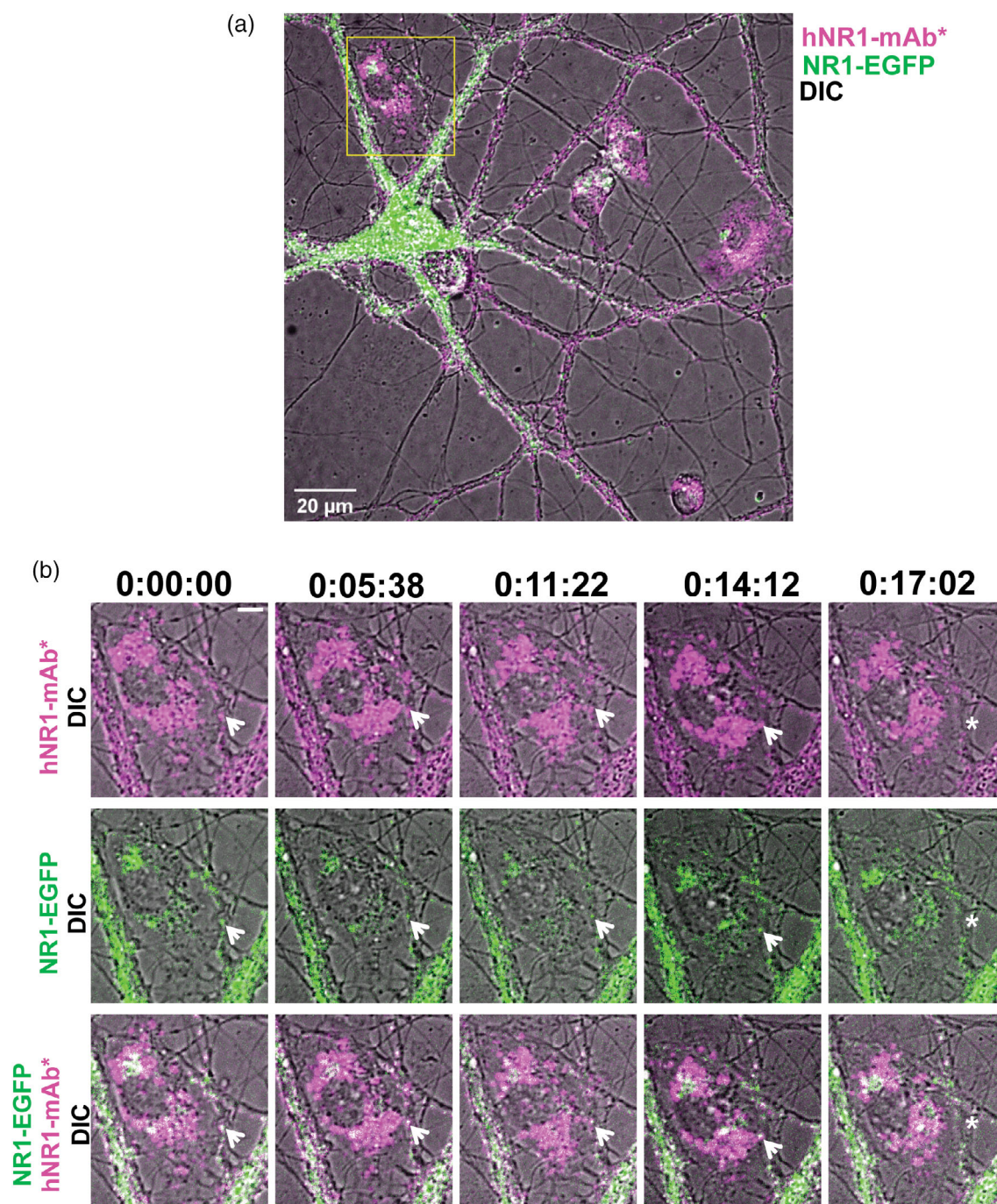


**FIGURE 4** Live imaging of microglia-mediated removal of NR1-EGFP/hNR1-mAb\* complexes from neurons. (a) Live cell imaging of NR1-EGFP (green) transfected hippocampal neurons with bound hNR1-mAb\* (magenta) co-cultured with microglia for 1 h before imaging for 1 h. DIC images were taken simultaneously to visualize axonal and dendritic branches and microglia. Yellow box represents zoomed ROI. (b) Time sequence images of selected ROI showing either hNR1-mAb\* (magenta), NR1-EGFP (green) or merge of NR1-EGFP/ hNR1-mAb\* (white) together with DIC at different time points. Arrow represents NR1-EGFP/ hNR1-mAb\* double positive puncta along a dendritic segment which over time ends up being lost from its location (asterisk) (~17 min) and taken up by an adjacent microglia with accumulated NR1-EGFP/ hNR1-mAb\* inside its cell body. Scale bar, 5 μm.

obtained for NR1-EGFP and hNR1-mAb\* (Figure 3e,f), we observed higher immunoreactivity for PSD95 (Figure 5e,f), but not vGLUT1 (Figure 5e,g), within microglia in the presence of bound NR1 autoantibody, implying that microglia can distinguish and

selectively removed antibody decorated sub-synaptic structures. Note, vGLUT1 only positive puncta could either represent orphan-presynaptic boutons or simply synaptic vesicle (SV) rich axonal varicosities (Krueger et al., 2003).

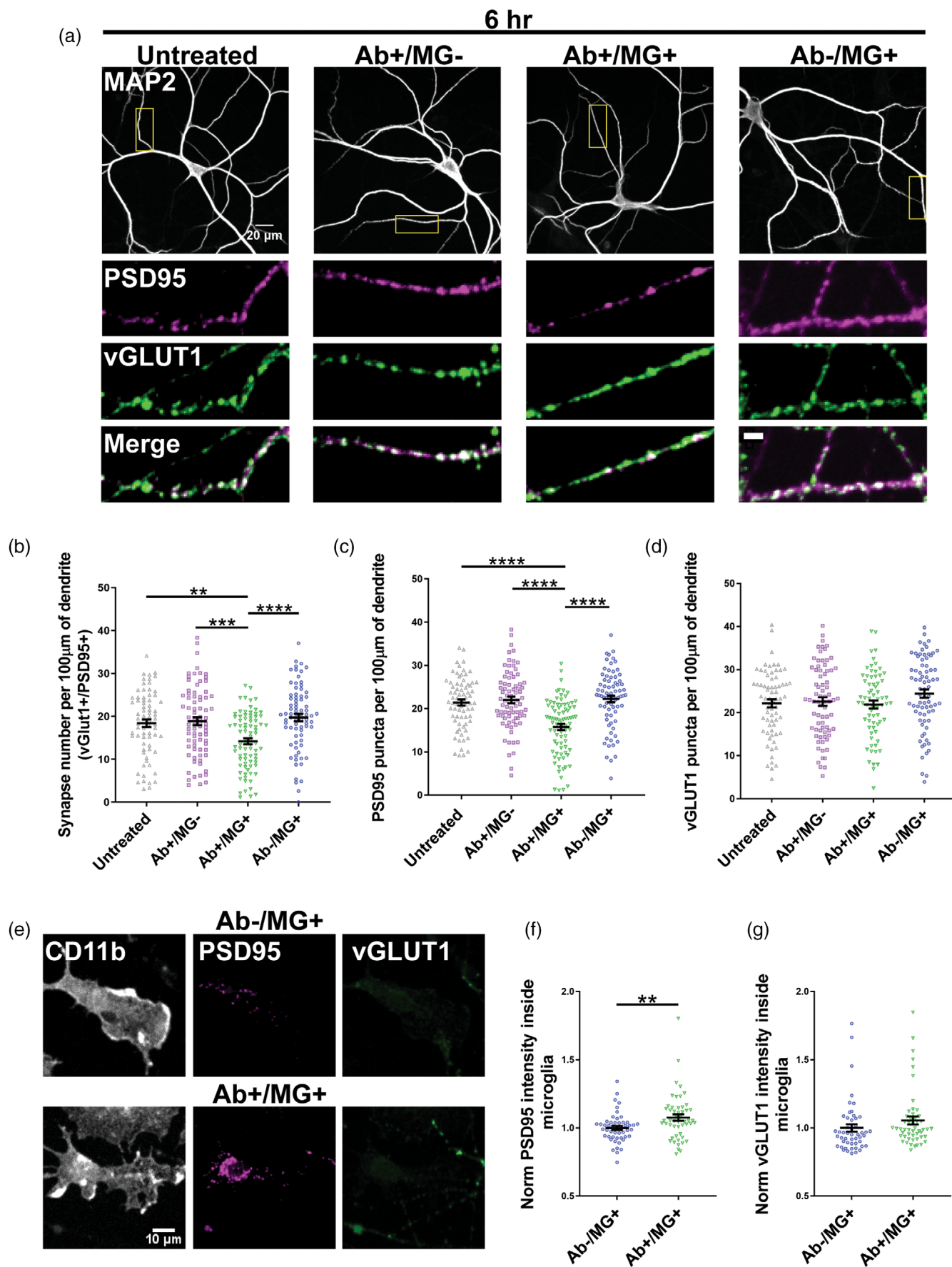


FIGURE 5 Legend on next page.



### 3.5 | hNR1-mAbs triggers microglia-mediated loss of different post-synaptic but not pre-synaptic reporters

To further explore the idea that microglia can selectively remove decorated post-synaptic components, we co-infected neurons with lentiviruses expressing different combinations of fluorescently tagged pre- and post-synaptic reporters (Homer-EGFP/mCherry-Synapsin or Synaptophysin-EGFP/PSD95-mKate2). Here, we observed a significant decrease in the number of Homer-EGFP ( $29.76 \pm 1.757$  for Ab<sup>+</sup>/MG<sup>-</sup> vs.  $22.33 \pm 1.381$  for Ab<sup>+</sup>/MG<sup>+</sup>,  $p = .0123$ ) (Figure 6a,b) or PSD95-mKate2 ( $26 \pm 0.8864$  for Ab<sup>+</sup>/MG<sup>-</sup> vs.  $17.67 \pm 1.179$  for Ab<sup>+</sup>/MG<sup>+</sup>,  $p < .0001$ ) (Figure 6d,e) positive puncta along dendrites, 6 h after co-culture with microglia in the presence of hNR1-mAb. However, no such decrease was observed in the number of mCherry-Synapsin ( $26.17 \pm 1.253$  for Ab<sup>+</sup>/MG<sup>-</sup> vs.  $26.18 \pm 1.282$  for Ab<sup>+</sup>/MG<sup>+</sup>,  $p > .999$ ) (Figure 6a,c) or Synaptophysin-EGFP ( $26.25 \pm 0.8186$  for Ab<sup>+</sup>/MG<sup>-</sup> vs.  $24.86 \pm 1.128$  for Ab<sup>+</sup>/MG<sup>+</sup>,  $p = .7552$ ) (Figure 6d,f) puncta. Importantly, no change in any post- and pre-synaptic markers was detected in any of the other experimental groups: that is, untreated, no microglia (Ab<sup>+</sup>/MG<sup>-</sup>) and no hNR1-mAb (Ab<sup>-</sup>/MG<sup>+</sup>). Thus, these results further indicate that hNR1-mAbs can selectively promote microglia-mediated removal of the post-synaptic material, but not necessarily the associated pre-synaptic proteins.

Furthermore, we utilized EM to test whether we see post-synaptic material within microglia after co-culture with hNR1-mAb bound hippocampal neurons. To this end, we utilized a lentivirus expressing Homer-EGFP to infect hippocampal neurons. Following hNR1-mAb addition to Homer-EGFP overexpressing neurons at (DIV 15–17), microglia were added for 90 min. The cells were then bleached, photo-converting EGFP in the presence of DAB, to a precipitate, before processing and EM imaging. EM micrographs revealed the presence of electron-dense material in membrane enclosed structures likely corresponding to multivesicular bodies or lysosomes containing photo-converted Homer-EGFP signal within microglia (Figures S5b and 5c). As in our antibody experiments (Figure S3) in

the absence of the hNR1-mAb (Ab<sup>-</sup>/MG<sup>+</sup>), the photo-converted DAB was largely restricted to mitochondria due to photo-conversion of reactive oxygen species that are generated during the mitochondrial ATP generation process (Figure S5a). This is in concordance with the loss of Homer-EGFP fluorescent puncta along dendrites of hNR1-mAb bound neurons in the presence of microglia, further supporting the observation that microglia remove post-synaptic components in presence of hNR1-mAb bound to neurons.

### 3.6 | Mutations blocking FcγR and complement binding of hNR1-mAb prevent autoantibody-driven removal of NMDARs

Next, we wanted to study the downstream mechanisms by which hNR1-mAb promotes removal of NMDARs and synapses by microglia. As mentioned above, it is known that the Fc region of IgG1 can be recognized by at least two immune cell associated receptors (FcγRs and complement receptors), promoting both immune cell activation and the clearance of antibody/antigen complexes (Bournazos et al., 2017). Thus theoretically, it should be possible to test for the contribution of each, by introducing mutations into the Fc region of hNR1-mAb that block their binding. In this regard, it has been reported that Leu234Ala/Leu235Ala (LALA) mutations can block Fcγ receptor binding, while a Pro329Ala (PA) mutation dampens complement activation. Moreover, a combination of these mutations (Leu234Ala/Leu235Ala/Pro329Gly) (LALA-PG) is expected to block binding of both (Lo et al., 2017; Saunders, 2019). We thus created recombinant version of the hNR1-mAb containing the LALA, PA or LALA-PG mutations (Figure S6a) that could be expressed and purified. These purified mutant hNR1-mAbs were initially tested for their antigen, FcγR and complement binding properties. Importantly, none of the mutations in the Fc region of the hNR1-mAb affected antigen binding, as each stained cultured hippocampal neurons in a punctate pattern that co-localized with vGLUT1 puncta along MAP2 positive dendrites, similar to the un-mutated WT antibody (Figure S6b). Importantly, these mutations affected the FcγRI (CD64) and complement

#### FIGURE 5 hNR1-mAb promotes microglia-mediated loss of post-synaptic proteins and synapses from neuron: Microglia co-cultures.

(a) Representative images of neurons either untreated (Ab<sup>-</sup>/MG<sup>-</sup>) or treated with Ab<sup>+</sup>/MG<sup>-</sup>, Ab<sup>+</sup>/MG<sup>+</sup> and Ab<sup>-</sup>/MG<sup>+</sup> before staining with MAP2 (gray), PSD95 or vGLUT1. Selected ROIs shows' staining's for PSD95 (magenta), vGLUT1 (green) and their merge (white) puncta along dendritic segments. Scale bar, 5 μm. (b) Quantification of synapse number (defined as vGLUT1<sup>+</sup>/PSD95<sup>+</sup> double positive puncta) per unit length of dendrite. A significant decrease vGLUT1<sup>+</sup>/PSD95<sup>+</sup> double positive puncta was only seen in the Ab<sup>+</sup>/MG<sup>+</sup> condition, 6 h after co-culture. Each data point represents an ROI from three independent experiments ( $n = 72$  for Ab<sup>-</sup>/MG<sup>-</sup>,  $n = 78$  for Ab<sup>+</sup>/MG<sup>-</sup>,  $n = 82$  for Ab<sup>+</sup>/MG<sup>+</sup> and  $n = 76$  for Ab<sup>-</sup>/MG<sup>+</sup>). Error bars represent SEM. One-way ANOVA with Tukey's multiple comparison test was used to evaluate statistical significance (\*\* $p = .0031$ ; \*\*\* $p = .0005$ ; \*\*\*\* $p < .0001$ ). (c) Quantification of PSD95 positive post-synaptic puncta per unit length of dendrite. A significant decrease was only seen in the Ab<sup>+</sup>/MG<sup>+</sup> condition after 6 h of co-culture, while the number of vGLUT1 pre-synaptic puncta per unit length of dendrite remained unchanged (d). Each data point represents an ROI from three independent experiments ( $n = 72$  for Ab<sup>-</sup>/MG<sup>-</sup>,  $n = 78$  for Ab<sup>+</sup>/MG<sup>-</sup>,  $n = 82$  for Ab<sup>+</sup>/MG<sup>+</sup> and  $n = 76$  for Ab<sup>-</sup>/MG<sup>+</sup>). Error bars represent SEM. One-way ANOVA with Tukey's multiple comparison test was used to evaluate statistical significance (\*\*\*\* $p < .0001$ ). (e) CD11b positive microglia (gray) images from Ab<sup>-</sup>/MG<sup>+</sup> and Ab<sup>+</sup>/MG<sup>+</sup> conditions after co-culture, reveals the accumulation of PSD95 (magenta) but not vGLUT1 (green) in microglia. (f and g) Normalized intensity of PSD95 increased while that of vGLUT1 remained unchanged inside microglia in Ab<sup>+</sup>/MG<sup>+</sup>, respectively, compared to Ab<sup>-</sup>/MG<sup>+</sup> condition. Each data point represents a microglia cell from three independent experiments ( $n = 50$  for Ab<sup>-</sup>/MG<sup>+</sup> and  $n = 51$  for Ab<sup>+</sup>/MG<sup>+</sup>). Error bars represent SEM. Unpaired t-test with Welch correction was used to evaluate statistical significance (\*\* $p = .0084$ ).



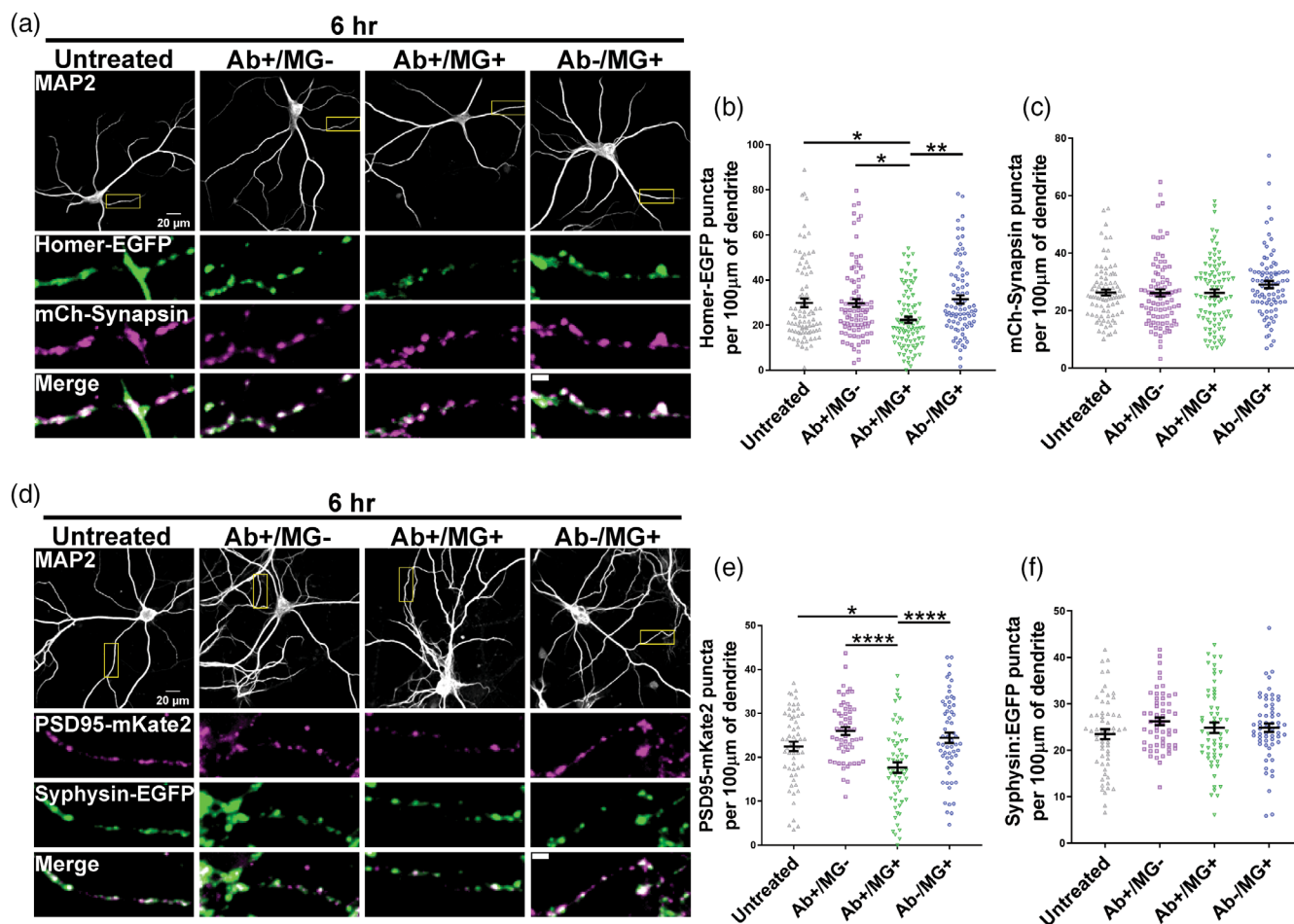


**FIGURE 6** Microglia promotes hNR1-mAb mediated loss of excitatory post-synaptic but not pre-synaptic proteins. (a) Representative images of MAP2 (gray) stained neurons overexpressing mCherry(mCh)-Synapsin and Homer-EGFP from Ab-/MG-, Ab+/MG-, Ab+/MG+ and Ab-/MG+ experimental conditions after 6 h. Selected ROIs reveals distribution and overlap (merge, white) of Homer-EGFP (green) and mCh-Synapsin (magenta) positive puncta along dendritic segments. Scale bar, 5  $\mu$ m. (b) Quantification of Homer-EGFP puncta number per unit length of dendrite, revealing a significant decrease only in the Ab+/MG+ condition, 6 h after co-culture. (c) Quantification of mCh-Synapsin puncta number per unit length of dendrite showed no change under any condition. Each data point represents an ROI from three independent experiments ( $n = 86$  for Ab-/MG-,  $n = 89$  for Ab+/MG-,  $n = 88$  for Ab+/MG+ and  $n = 83$  for Ab-/MG+). Error bars represent SEM. One-way ANOVA with Tukey's multiple comparison test was used to evaluate statistical significance (\* $p = .0118$ ; \*\* $p = .0014$ ). (D) Representative images of MAP2 stained (gray) neurons overexpressing Synaptophysin-EGFP (Syphysin-EGFP) and PSD95-mKate2 from Ab-/MG-, Ab+/MG-, Ab+/MG+ and Ab-/MG+ experimental conditions, after 6 h. Selected ROIs show staining's for PSD95-mKate2 (magenta), Syphysin-EGFP (green) and their merge (white) puncta along dendritic segments. Scale bar, 5  $\mu$ m (e) and (f) PSD95-mKate2 puncta along dendritic segments decreased only in Ab+/MG+ condition while that of Syphysin-EGFP remains unchanged, respectively. Each data point represents an ROI from two independent experiments ( $n = 58$  for Ab-/MG-,  $n = 57$  for Ab+/MG-,  $n = 59$  for Ab+/MG+ and  $n = 60$  for Ab-/MG+). Error bars represent SEM. One-way ANOVA with Tukey's multiple comparison test was used to evaluate statistical significance. (\* $p = .0114$ ; \*\*\*\* $p < .0001$ )

binding of the hNR1-mAb (Figure S6c,d). Surprisingly, all the mutants, that is, LALA, PA and LALA-PG had reduced Fc $\gamma$ RI and C1q binding compared to the WT-hNR1-mAb in binding assays (Figure S6c,d). Of note the double mutant LALA-PG appeared to bind least well (Figure S6c,d). Unfortunately, these mutations reduced binding to both Fc $\gamma$ RI and C1q, with little specificity over either receptor, an observation also reported by others (Schlothauer et al., 2016), precluding our ability to assess the individual contribution of each.

To assess the functional impact of the Fc $\gamma$ RI and C1q binding mutations on microglia-mediated NMDAR removal, we utilized each in our neuron/microglia co-culture assay, during which each was

added at 2  $\mu$ g/mL, unlabeled to pre-labeled in 1:1 ratio, for 30 min before washing and adding microglia for 6 h. Here, we observed a significant decrease in the number of hNR1-mAb puncta along dendrites after 6 h only when WT hNR1-mAb\* was used in co-culture ( $23.04 \pm 1.245$  for Ab+/MG- vs.  $16.3 \pm 0.9746$  for Ab+/MG+,  $p < .0001$ ) (Figure 7a,e). No such decrease was seen for LALA-PG ( $24.03 \pm 0.9874$  for Ab+/MG- vs.  $22.51 \pm 1.189$  for Ab+/MG+,  $p = .3281$ ) (Figure 7b,f), LALA ( $27.17 \pm 0.7405$  for Ab+/MG- vs.  $26.69 \pm 0.9778$  for Ab+/MG+,  $p = .6976$ ) (Figure 7c,g) or PA ( $25.56 \pm 0.9195$  for Ab+/MG- vs.  $25.84 \pm 0.9657$  for Ab+/MG+,  $p = .8358$ ) (Figure 7d,h) mutants of hNR1-mAb\*. On analyzing

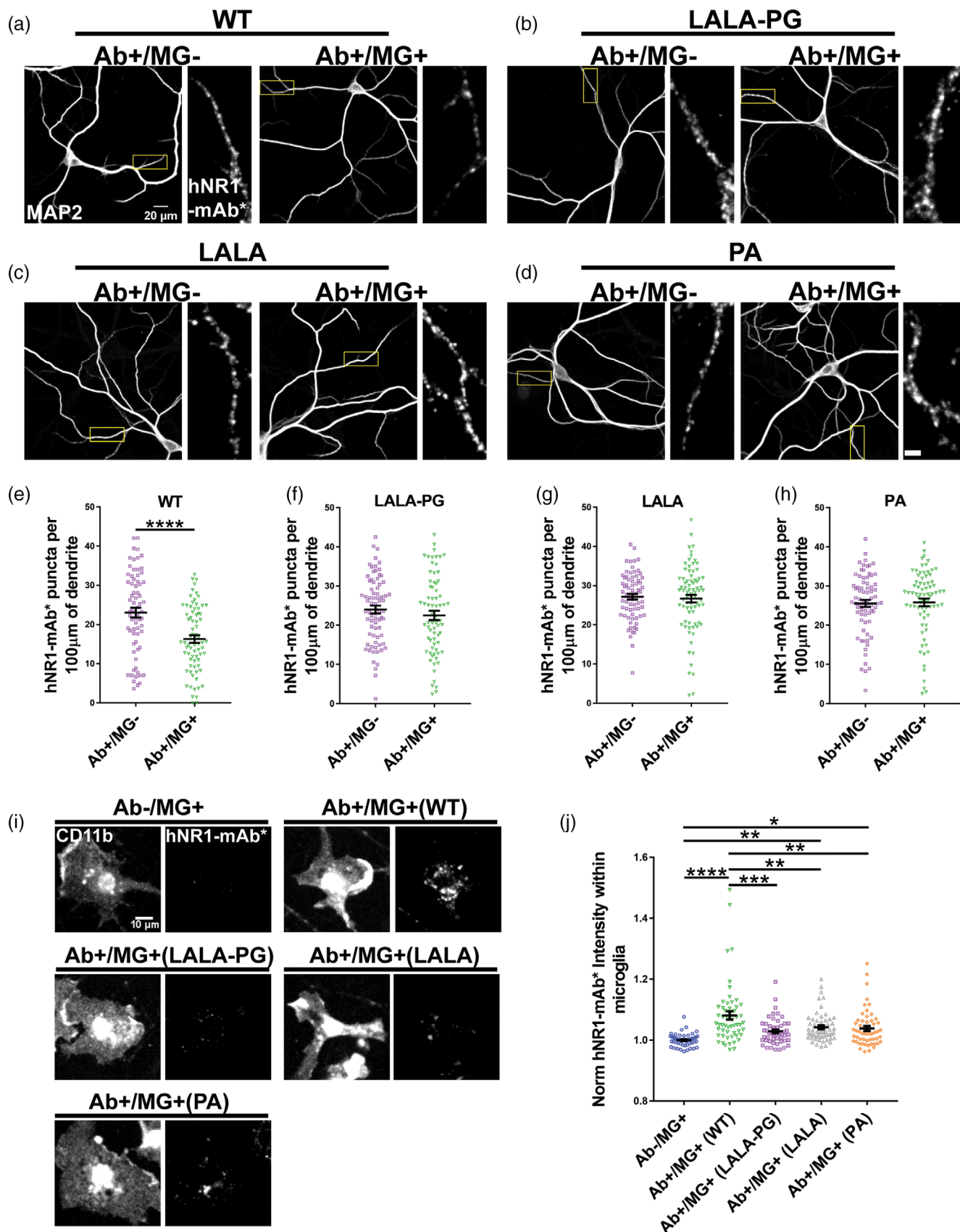


**FIGURE 7** Legend on next page.

microglia from these co-culture experiments, significantly higher fluorescence intensities of antibody labeled puncta were found in CD11b positive microglia from co-cultures with WT hNR1-mAb\*, while no appreciable increase was seen for the LALA-PG mutant ( $1 \pm 0.0028$  for Ab-/MG+,  $1.081 \pm 0.0137$  for Ab+/MG+ (WT);  $p < .0001$ ,  $1.029 \pm 0.0059$  (LALA-PG);  $p = .1255$ ) (Figure 7i,j). Even though less than WT, both LALA ( $1 \pm 0.0028$  for Ab-/MG+ vs.  $1.042 \pm 0.0064$  for Ab+/MG+(LALA),  $p = .0041$ ) and PA ( $1 \pm 0.0028$  for Ab-/MG+ vs.  $1.038 \pm 0.01028$  for Ab+/MG+(PA),  $p = .0127$ ) mutant antibodies exhibited detectable, yet low levels inside microglia (Figure 7i,j), suggesting some limited microglia receptor engagement, though without overt effects on hNR1-mAb\* puncta number per unit length of dendrite (Figure 7g,h).

As the LALA and PA mutants did not allow us to cleanly separate FcγR from complement-mediated microglia engagement, we explored whether the stronger LALA-PG hNR1-mAb mutant (unlabeled) impairs microglia-mediated synapse loss in our co-culture system. This was initially accomplished by immuno-staining cultures with antibodies against vGLUT1 and PSD95 and then quantifying changes in puncta number and degree of co-localization. Here, we observed a decrease in the number of PSD95 positive puncta/unit length of dendrite ( $18.4 \pm 0.9871$  for Ab+/MG- vs.  $13.32 \pm 0.8324$  for Ab+/MG+,  $p = .0005$ ) (Figure 8c) and a similar decrease in the number of vGLUT1+/PSD95+ double positive puncta/unit length of dendrite ( $18.4 \pm 0.9871$  for Ab+/MG- vs.  $13.32 \pm 0.8324$  for Ab+/MG+,  $p < .0033$ ) (Figure 8b) 6 h after co-culturing microglia with neurons in presence of WT hNR1-mAb (Figure 8a). No such loss of synapses (vGLUT1+/PSD95+ double positive puncta) ( $19.65 \pm 0.9473$  for Ab+/MG- vs.  $20.53 \pm 0.9895$  for Ab+/MG+,  $p = .9846$ ) (Figure 8b) or post-synaptic PSD95 puncta ( $22.21 \pm 0.9734$  for Ab+/MG- vs.  $23.62 \pm 0.9876$  for Ab+/MG+,  $p = .8844$ ) (Figure 8c) was observed when the LALA-PGhNR1-mAb mutant was pre-bound to the neurons in our co-culture system (Figure 8c). The number of vGLUT1 positive puncta/unit length of dendrite remained the same for all experimental groups irrespective of whether WT or LALA-PG hNR1-mAb was present in the co-culture (Figure 8d). Consistent with this, immunostaining of PSD95 was found to be significantly higher

inside microglia 6 h after co-culturing with neurons pre-bound with the WT hNR1-mAb (Figure 8e,f). Such an increase was not seen for vGLUT1 inside microglia with either WT or LALA-PG hNR1-mAb (Figure 8e,g). These data indicate that the stripping of NMDARs and post-synaptic entities by microglia requires the engagement of auto-antibodies with FcγRs and/or complement receptors.

### 3.7 | Microglia-mediated removal of autoantibody-tagged receptors is selective

Conceptually, autoantibodies bound to neuronal receptors could either trigger microglia-mediated removal of specific receptors or through a general activation of microglia causing the unspecific upregulation of phagocytosis activity and indiscriminate removal of different receptors. To explore these options, we used another patient-derived monoclonal autoantibody that selectively binds α1 subunit of the GABA<sub>A</sub> receptor (α1-GABA<sub>A</sub>R-mAb) in our co-culture setup. Initially, we investigated whether α1-GABA<sub>A</sub>R-mAb, labeled with the Zenon-kit (Alexa 647) (α1-GABA<sub>A</sub>R-mAb\*), also induced microglia dependent removal of GABA<sub>A</sub>Rs (Figure 9a). As above, labeled antibody was mixed 1:1 with unlabeled antibody (α1-GABA<sub>A</sub>R-mAb\*/α1-GABA<sub>A</sub>R-mAb). Here, we observed a significant decrease in α1-GABA<sub>A</sub>R-mAb\* positive puncta along dendrites ( $21.88 \pm 0.9537$  for Ab+/MG- vs.  $11.34 \pm 1.001$  for Ab+/MG+,  $p < .0001$ ) (Figure 9b), 6 h after co-culture. Increased fluorescence from α1-GABA<sub>A</sub>R-mAb\* also seen within CD11b positive microglia (Figure 9c,d). Interestingly, we observed a higher intensity of α1-GABA<sub>A</sub>R-mAb\* puncta/fluorescence within microglia compared to NMDAR/NR1-mAb\* (Figure S7a,b) even though the number of respective puncta/unit length of dendrite lost remained similar (Figure S7c). This is consistent with the high levels of expression of synaptic α1-GABA<sub>A</sub>Rs compared to NR1/NMDARs in hippocampal cultures as reported previously (Behuet et al., 2019). Next, we utilized both the α1-GABA<sub>A</sub>R-mAb and hNR1-mAb antibodies in the co-culture experiment to check for specificity of microglia-mediated removal of autoantibody tagged receptors. Initially, this was

**FIGURE 7** FcγR and C1q mutant hNR1-mAbs prevent microglia-mediated loss of NMDARs. (a–d) Representative images of neurons stained for MAP2 (gray) from Ab+/MG-, Ab+/MG+ experimental conditions after pre-labeling with either WT, LALA-PG, LALA or PA hNR1-mAb\*. Selected ROIs shows hNR1-mAb\* puncta (white) along dendritic segments for each of the Fc region mutant of hNR1-mAb. Scale bar, 5 μm. (e–h) Quantification of the number of hNR1-mAb\* puncta per unit length of dendrite in the presence (Ab+/MG+) or absence (Ab+/MG-) of microglia. There was a significant decrease in the number of WT hNR1-mAb puncta, but not mutant antibodies (LALA-PG, LALA and PA) under Ab+/MG+ condition 6 h after co-culture. Each data point represents an ROI from three independent experiments ( $n = 70$  for Ab+/MG- and  $n = 74$  for Ab+/MG+) (WT hNR1-mAb,  $n = 70$  for Ab+/MG- and  $n = 74$  for Ab+/MG+) (LALA-PG hNR1-mAb,  $n = 75$  for Ab+/MG- and  $n = 72$  for Ab+/MG+) (LALA hNR1-mAb,  $n = 70$  for Ab+/MG- and  $n = 78$  for Ab+/MG+) (PA hNR1-mAb,  $n = 73$  for Ab+/MG- and  $n = 77$  for Ab+/MG+). Error bars represent SEM. Unpaired t-test was used to evaluate statistical significance (\*\*\*\* $p < .0001$ ). For LALA hNR1-mAb\* unpaired t-test with Welch correction was used to evaluate statistical significance as the variances were different within experimental groups. (i) Images of CD11b positive microglia with hNR1-mAb\* immunoreactivity with or without different hNR1-mAb\* (WT, LALA-PG, LALA or PA hNR1-mAb\*) after co-culture for 6 h. Images presented in grayscale. (j) Normalized quantification of hNR1-mAb\* intensity within microglia is significantly higher in Ab+/MG+ group for WT, LALA and PA hNR1-mAb\* than Ab-/MG+ group. No such increase was seen in Ab+/MG+ group with LALA-PG hNR1-mAb bound to neurons after 6 h of co-culture. Each data point represents a microglia cell from three independent experiments ( $n = 52$ – $56$  for each experimental group). Error bars represent SEM. One-way ANOVA with Tukey's multiple comparison test was used to evaluate statistical significance (\* $p = .0127$ ; \*\* $p < .005$ ; \*\*\* $p = .0001$ ; \*\*\*\* $p < .0001$ ).



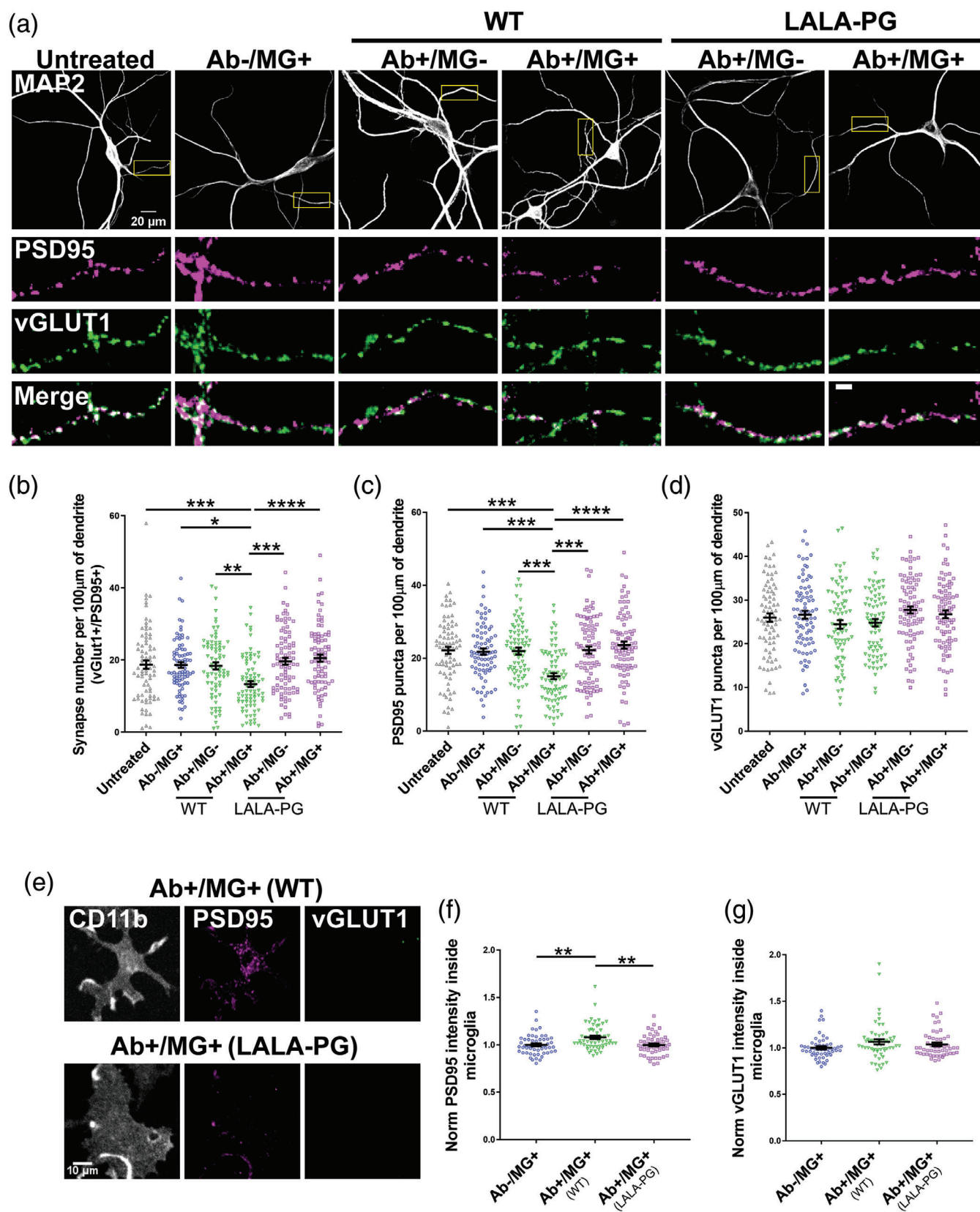


**FIGURE 8** Legend on next page.

performed in a sequential labeling experiment, wherein microglia were added for 6 h to neurons pre-labeled with  $\alpha 1$ -GABA<sub>A</sub>R-mAb\* (Alexa 647)/ $\alpha 1$ -GABA<sub>A</sub>R-mAb for 30 min (Figure 9e), followed by the addition of hNR1-mAb\* (Alexa 594) for 30 min before fixation. Here, we observed the expected decrease of number of  $\alpha 1$ -GABA<sub>A</sub>R-mAb\*/unit length of dendrite from the surface of neurons ( $25.63 \pm 1.0190$  for Ab+/MG– vs.  $18.22 \pm 0.8333$  for Ab+/MG+,  $p < .0001$ ) (Figure 9f), with no decrease in the number of hNR1-mAb\* positive puncta/unit length of dendrite ( $24.6 \pm 0.8008$  for Ab+/MG– vs.  $24.7 \pm 0.8437$  for Ab+/MG+,  $p = .9340$ ) (Figure 9g). To further validate this selective microglial action, we performed the converse experiment, wherein neuronal cultures were initially labeled with hNR1-mAb\* (Alexa 647)/hNR1-mAb for 30 min before the addition of microglia for 6 h. Subsequently, co-cultures were labeled with  $\alpha 1$ -GABA<sub>A</sub>R-mAb\* (Alexa 594) for 30 min fixed and imaged (Figure 9h). Again, we observed a significant decrease in hNR1-mAb\* puncta ( $26.83 \pm 1.006$  for Ab+/MG– vs.  $17.38 \pm 0.8523$  for Ab+/MG+,  $p < .0001$ ) (Figure 9i), while the number of  $\alpha 1$ -GABA<sub>A</sub>R-mAb\* puncta/unit length of dendrite remained unchanged ( $24.37 \pm 1.032$  for Ab+/MG– vs.  $25.74 \pm 0.9905$  for Ab+/MG+,  $p = .3397$ ) (Figure 9j). These data indicate that microglia can selectively remove autoantibody-tagged receptors and do not necessarily cause an unspecific removal of other neuronal receptors.

To explore this concept further, we examined whether microglia can distinguish between two antibodies added simultaneously. This allowed us to also compare the importance of the Fc region by pairing WT and LALA-PG mutant antibodies. This was accomplished by co-labeling neuronal culture for 30 min, with  $\alpha 1$ -GABA<sub>A</sub>R-mAb\*/ $\alpha 1$ -GABA<sub>A</sub>R-mAb together with either the WT (Figure 10a) or LALA-PG mutant (Figure 10d) of the hNR1-mAb\*/hNR1-mAb, before washing and adding microglia. When  $\alpha 1$ -GABA<sub>A</sub>R-mAb\* and WT hNR1-mAb\* were simultaneously bound to neurons and microglia then added for 6 h, we detected a significant reduction in the number of both  $\alpha 1$ -GABA<sub>A</sub>R-mAb\* ( $22.06 \pm 0.8494$  for Ab+/MG– vs.  $14.09 \pm 0.9742$  for Ab+/MG+,  $p < .0001$ ) (Figure 10b) and hNR1-mAb\* ( $23.9 \pm 1.131$  for Ab+/MG– vs.  $14.42 \pm 0.9521$  for Ab+/MG+,  $p < .0001$ ) (Figure 10c) puncta along dendrites.

However, when  $\alpha 1$ -GABA<sub>A</sub>R-mAb\* and LALA-PG hNR1-mAb\* were present together in co-culture, there was a selective loss of  $\alpha 1$ -GABA<sub>A</sub>R-mAb\* puncta ( $22.18 \pm 1.248$  for Ab+/MG– vs.  $13.19 \pm 1.013$  for Ab+/MG+,  $p < .0001$ ) (Figure 10e) from the surface of neurons, while the number of LALA-PG hNR1-mAb\* puncta remained unchanged ( $25.68 \pm 1.143$  for Ab+/MG– vs.  $27.37 \pm 1.507$  for Ab+/MG+,  $p = .3719$ ) (Figure 10f). Taken together, these results indicate that microglia selectively remove autoantibody-tagged receptors via functional FcγRI and C1q binding sites within the Fc regions of these antibodies.

## 4 | DISCUSSION

Autoantibodies, implicated in autoimmune encephalitis, have been shown to employ different mechanisms leading to pathogenic outcomes. These include binding and blocking receptor function like GABA<sub>B</sub>R (Dalmay & Graus, 2018) and GlyR (Rauschenberger et al., 2020), triggering receptor crosslinking driven internalization, like NMDAR (Hughes et al., 2010; Kreye et al., 2016) and inhibiting receptor ligand interaction like in leucine-rich glioma-inactivated 1 (LGI1) (Kornau et al., 2020; Ohkawa et al., 2013). Additionally, autoantibodies can also lead to inflammation and cell death via complement activation, for example, AQP4 (Sabater et al., 2009; Soltys et al., 2019). However, the role of encephalitis patient-derived autoantibodies in activating resident and infiltrating immune cells of the CNS through FcγR binding and non-classical pathway of complement mediated opsonisation of antigen remains largely unexplored.

In this study, using patient-derived recombinant hNR1-mAb in a neuron/microglia co-culture setup, we report that hNR1-mAb bound to NMDARs led to microglia engagement and loss of NMDAR/hNR1-mAb complexes from hippocampal neurons (Figure 3a–c). Concomitantly, these complexes appeared to accumulate within CD11b positive microglia (Figure 3c,d) inside Lamp2a+ and CD68+ lysosomal compartments (Figure 2e,f). The receptor removal was specific to the NR1 autoantibody-bound NMDARs, as we did not observe changes in

**FIGURE 8** LALA-PG hNR1-mAb mutant prevents microglia-mediated synapse loss. (a) Representative images of neurons stained for MAP2 (gray) from untreated (Ab–/MG–), Ab+/MG–, Ab+/MG+ and Ab–/MG+ experimental groups for both WT and LALA-PG hNR1-mAb after 6 h. Selected ROIs shows immune-staining for PSD95 (magenta), vGLUT1 (green) and their merge (white) puncta along dendritic segments. Scale bar, 5 μm. (b) Quantification of the number of synapses (vGLUT1+/PSD95+ puncta) per unit length of dendrite. Data show a significant decrease only in synapse number with the WT hNR1-mAb containing Ab+/MG+ group 6 h after co-culture. Each data point represents an ROI from three independent experiments ( $n = 78$  for Ab–/MG–,  $n = 82$  Ab–/MG+,  $n = 78$  for Ab+/MG–;  $n = 80$  for Ab+/MG+ for WT hNR1-mAb,  $n = 87$  for Ab+/MG–;  $n = 85$  for Ab+/MG+ for LALA-PG hNR1-mAb). Error bars represent SEM. One-way ANOVA with Tukey's multiple comparison test was used to evaluate statistical significance (\*\* $p < .003$ ; \*\*\* $p < .00001$ ). (c) Quantification of the number of PSD95 puncta per unit length of dendrite. Data reveal a decrease PSD95 puncta number in the WT hNR1-mAb containing Ab+/MG+ group after 6 h of co-culture, while the number of vGLUT1 pre-synaptic puncta remains unchanged in all experimental groups (d). Each data point represents an ROI from three independent experiments ( $n = 78$  for Ab–/MG–,  $n = 82$  Ab–/MG+,  $n = 78$  for Ab+/MG–;  $n = 80$  for Ab+/MG+ for WT hNR1-mAb,  $n = 87$  for Ab+/MG–;  $n = 85$  for Ab+/MG+ for LALA-PG hNR1-mAb). Error bars represent SEM. One-way ANOVA with Tukey's multiple comparison test was used to evaluate statistical significance (\*\*\*\* $p < .00001$ ). (e) Images of microglia labeled with CD11b (gray) showing an increase PSD95 (magenta) staining inside microglia in WT hNR1-mAb treated group (Ab+/MG+) as compared to LALA-PG (Ab+/MG+) group. No significant staining for vGLUT1 (green) was observed inside microglia for any experimental group. Each data point represents a microglia cell from three independent experiments ( $n = 53$  for Ab–/MG+,  $n = 57$  for WT hNR1-mAb Ab+/MG+,  $n = 51$  for LALA-PG hNR1-mAb Ab+/MG+). Error bars represent SEM. One-way ANOVA with Tukey's multiple comparison test was used to evaluate statistical significance (\*\* $p < .005$ ).





GABA<sub>A</sub>R numbers after addition of microglia (Figure 9h–j). Similar results were obtained with a second patient-derived monoclonal against GABA<sub>A</sub>Rs. Here, again the  $\alpha 1$ -GABA<sub>A</sub>R-mAb triggered a significant decrease in GABA<sub>A</sub>R puncta 6 h after microglia addition, without changes in the number of NMDARs (Figure 9e–g).

Hence, we could show that antibody-dependent removal of receptors by microglia can be specific to the bound antibody and its target receptor.

Gestational transfer of patient-derived NR1-Abs was recently reported to cause a reduction in number of synapses as well as

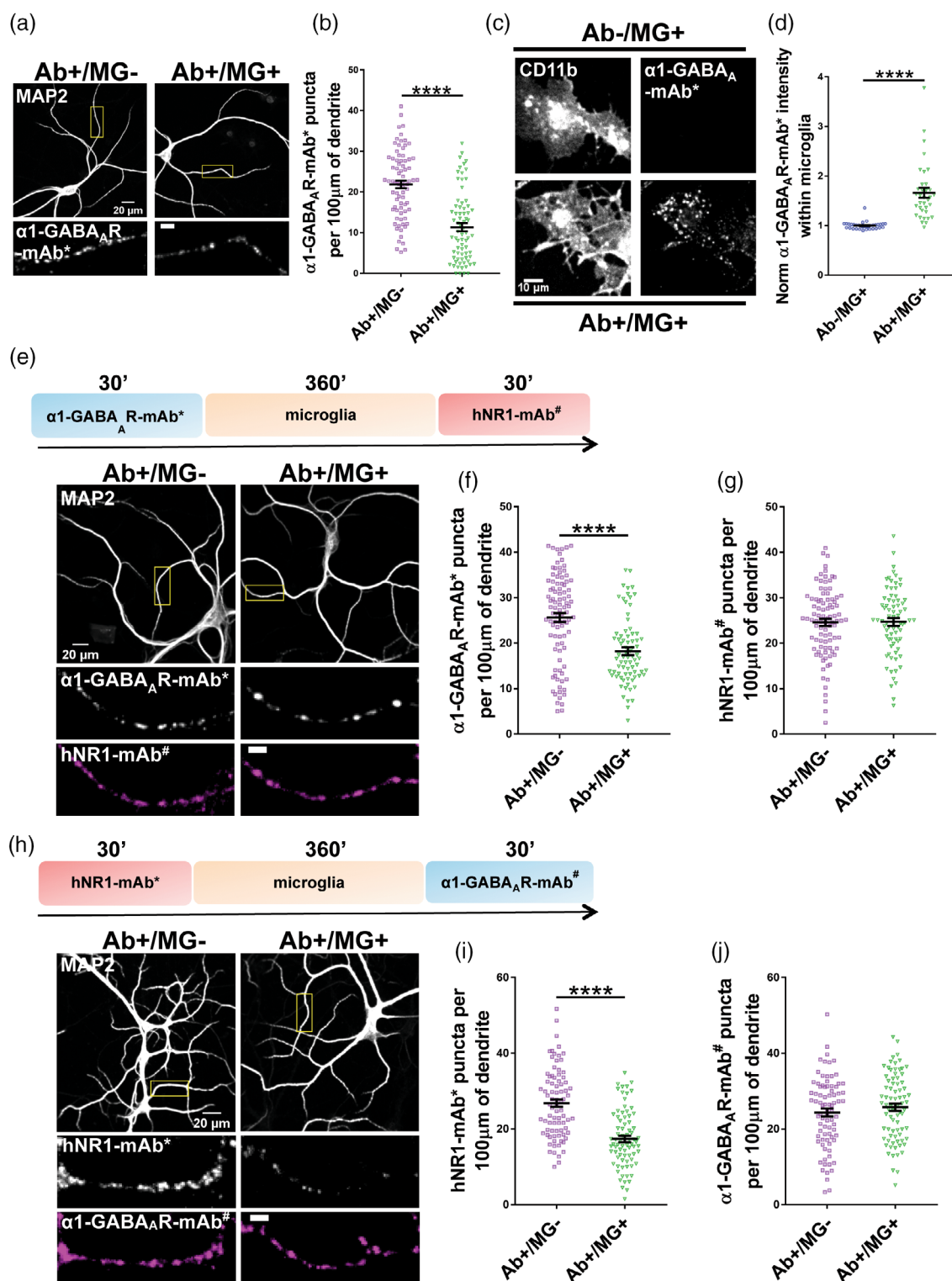


FIGURE 9 Legend on next page.

microglial activation in the hippocampus of postnatal mice following intrauterine exposure to patient IgGs (García-Serra et al., 2021). Consistent with a role of microglia in this clearance, we observed a significant decrease in the number of synapses 6 h after the addition of microglia to hNR1-mAb bound hippocampal neurons (Figure 5). Intriguingly, we observed a specific loss of post-synaptic markers like PSD95 and Homer1 without changes in markers of pre-synapse like vGLUT1, Synapsin1 and Synaptophysin, (Figures 5 and 6) which could be due to a majority of NMDARs being localized post-synaptically (Ehlers et al., 1995; Zhang et al., 2013). It should be noted that while significant changes in synaptic number was only detected after 6 h, microglia were capable in live-imaging and EM experiments of removing such complexes within the first hour. This delay would be related to the kinetics of synapse removal, migration rates of microglia and total number of labeled synapses.

Previous studies have reported the role of microglia in synapse pruning during development (Paolicelli et al., 2011; Schafer et al., 2012) and in neurodegenerative disorders like Alzheimer's disease (Hong et al., 2016; Rajendran & Paolicelli, 2018). Interestingly, others have shown that oligomeric amyloid beta ( $\alpha\text{A}\beta$ ) localizes to post-synapses (Koffie et al., 2009; Lacor et al., 2004) and that such a post-synaptic localization requires NMDARs (Decker et al., 2010; Li et al., 2011). This  $\alpha\text{A}\beta$  localization at post-synapses has been reported to trigger microglia dependent removal of synapses, more intriguingly, only post-synapses, via post-synaptic complement deposition, in pre-plaque brains (3–4 months post-natal) of APP/PS1 mice (Hong et al., 2016). These studies add to our observation that hNR1-mAb bound NMDARs can cause microglia to selectively remove post-synaptic components. However, here we could not distinguish between whether microglia in the presence of bound hNR1-mAb removes only NMDAR associated post-synaptic proteins or the entire

post-synaptic density (PSD), leaving behind previously reported orphan synapses with just the associated pre-synaptic bouton (Krueger et al., 2003; Liberman & Liberman, 2015). Another important unanswered question in our study is whether microglia can access the synaptic cleft to remove the whole post-synaptic density or whether hNR1-mAbs, or other pathogenic proteins like  $\alpha\text{A}\beta$ , first promote the lateral movement of receptors and different post-synaptic proteins into an extra synaptic space, from where they are more accessible for microglia-mediated clearance. Further work will be needed to address this important question.

Several studies have investigated the potential of antibody against self and non-self antigens to engage and activate immune cells. For example, monoclonal antibodies targeting specific cancer-associated proteins have been shown to bind Fc $\gamma$ Rs on macrophages leading to antibody-dependent cellular phagocytosis (ADCP), thereby killing tumor cells (Scott et al., 2012; Zhou et al., 2020). Similarly, auto-antibodies involved in Inflammatory Rheumatoid Arthritis (IRA) have been reported to activate non-classical mode of complement activation (Ji et al., 2002), as well as engage Fc $\gamma$ Rs on macrophages leading to release of inflammatory cytokines like IL-6, IL-1 $\beta$  and TNF $\alpha$  (Ludwig et al., 2017) that increase osteoclast activity, ultimately reducing bone density (Zuo & Deng, 2021). Within CNS, antibodies against myelin oligodendrocyte glycoprotein (MOG) have been observed to promote the uptake and presentation of MOG via binding to Fc $\gamma$ Rs on myeloid antigen presenting cells (APCs), that is, macrophages and dendritic cells and resident phagocytes of the CNS, that is, microglia and astrocytes thereby leading to enhanced effector T cell engagement (Flach et al., 2016; Kinzel et al., 2016). In neuromyelitis optica (NMO), AQP4 reactive IgG resulted in microglia/macrophage reactivity in lesions along with complement activation (Lucchinetti et al., 2014). Furthermore, in microglia ablation studies wherein

**FIGURE 9** Microglia selectively removes only autoantibody-bound receptors. (a) Images of MAP2 (gray) stained hippocampal neurons pre-labeled with  $\alpha 1$ -GABA<sub>A</sub>R-mAb\* (Alexa647) with or without microglia addition (i.e., Ab+/MG+ and Ab+/MG−) after 6 h. Selected ROIs shows immuno-staining for  $\alpha 1$ -GABA<sub>A</sub>R-mAb\* puncta (white) along dendritic segments. Scale bar, 5  $\mu$ m. (b) Quantification of the number of  $\alpha 1$ -GABA<sub>A</sub>R-mAb\* puncta per unit length of dendrite reveals decrease in Ab+/MG+ group 6 h after co-culture. Each data point represents an ROI from three independent experiments ( $n = 77$  for Ab+/MG−,  $n = 73$  Ab+/MG+). Error bars represent SEM. Unpaired  $t$ -test was used to evaluate statistical significance (\*\*\*\* $p < .00001$ ). (c) CD11b positive microglia with accumulated  $\alpha 1$ -GABA<sub>A</sub>R-mAb\* immunoreactivity in Ab+/MG+ but not Ab−/MG+ condition. Images represented in grayscale. (d) Normalized intensity of  $\alpha 1$ -GABA<sub>A</sub>R-mAb\* fluorescence inside microglia was higher in Ab+/MG+ over Ab−/MG+ condition. Each data point represents a microglial cell over three independent experiments ( $n = 35$  for Ab−/MG+,  $n = 35$  Ab+/MG+). Error bars represent SEM. Unpaired  $t$ -test with Welch correction was used to evaluate statistical significance (\*\*\*\* $p < .00001$ ). (e) Representative images of neurons with MAP2 staining (gray) with bound  $\alpha 1$ -GABA<sub>A</sub>R-mAb\* (Alexa647) with or without microglia addition for 6 h. Upper panel is a schematic of the experimental setup. Pre-labeled hNR1-mAb\* (Alexa 594) was added for 30 min after the 6 h microglia incubation. ROIs shows  $\alpha 1$ -GABA<sub>A</sub>R-mAb\* (white) and hNR1-mAb\* (magenta) puncta along dendritic segments. Scale bar, 5  $\mu$ m. (f) Quantification of  $\alpha 1$ -GABA<sub>A</sub>R-mAb\* puncta number per unit length of dendrite reveals a significant reduction in puncta number in the presence of microglia Ab+/MG+. (g) The number of hNR1-mAb\* puncta per unit length of dendrite did not change. Each data point represents an ROI from three independent experiments ( $n = 94$  for Ab+/MG−,  $n = 78$  for Ab+/MG+). Error bars represent SEM. Unpaired  $t$ -test was used to evaluate statistical significance (\*\*\*\* $p < .00001$ ). Unpaired  $t$ -test with Welch correction was used to evaluate statistical significance for hNR1-mAb\* puncta per unit length. (h) Representative images of MAP2 stained neurons (gray) with bound hNR1-mAb\* (Alexa 647) with or without microglia addition for 6 h. Pre-labeled  $\alpha 1$ -GABA<sub>A</sub>R-mAb\* (Alexa 594) was added for 30 min after 6 h. Upper panel is a schematic of the experimental setup. ROIs shows hNR1-mAb\* (white) and  $\alpha 1$ -GABA<sub>A</sub>R-mAb\* (magenta) puncta along dendritic segments. Scale bar, 5  $\mu$ m. (i, j) Quantitation of hNR1-mAb\* or  $\alpha 1$ -GABA<sub>A</sub>R-mAb\* puncta per unit length of dendrite. hNR1-mAb\* puncta number was significantly reduced in presence of microglia Ab+/MG+, while the number of  $\alpha 1$ -GABA<sub>A</sub>R-mAb\* puncta per unit length of dendrite did not change. Each data point represents an ROI from three independent experiments ( $n = 82$  for Ab+/MG−,  $n = 78$  for Ab+/MG+). Error bars represent SEM. Unpaired  $t$ -test with Welch correction was used to evaluate statistical significance (\*\*\*\* $p < .00001$ ).

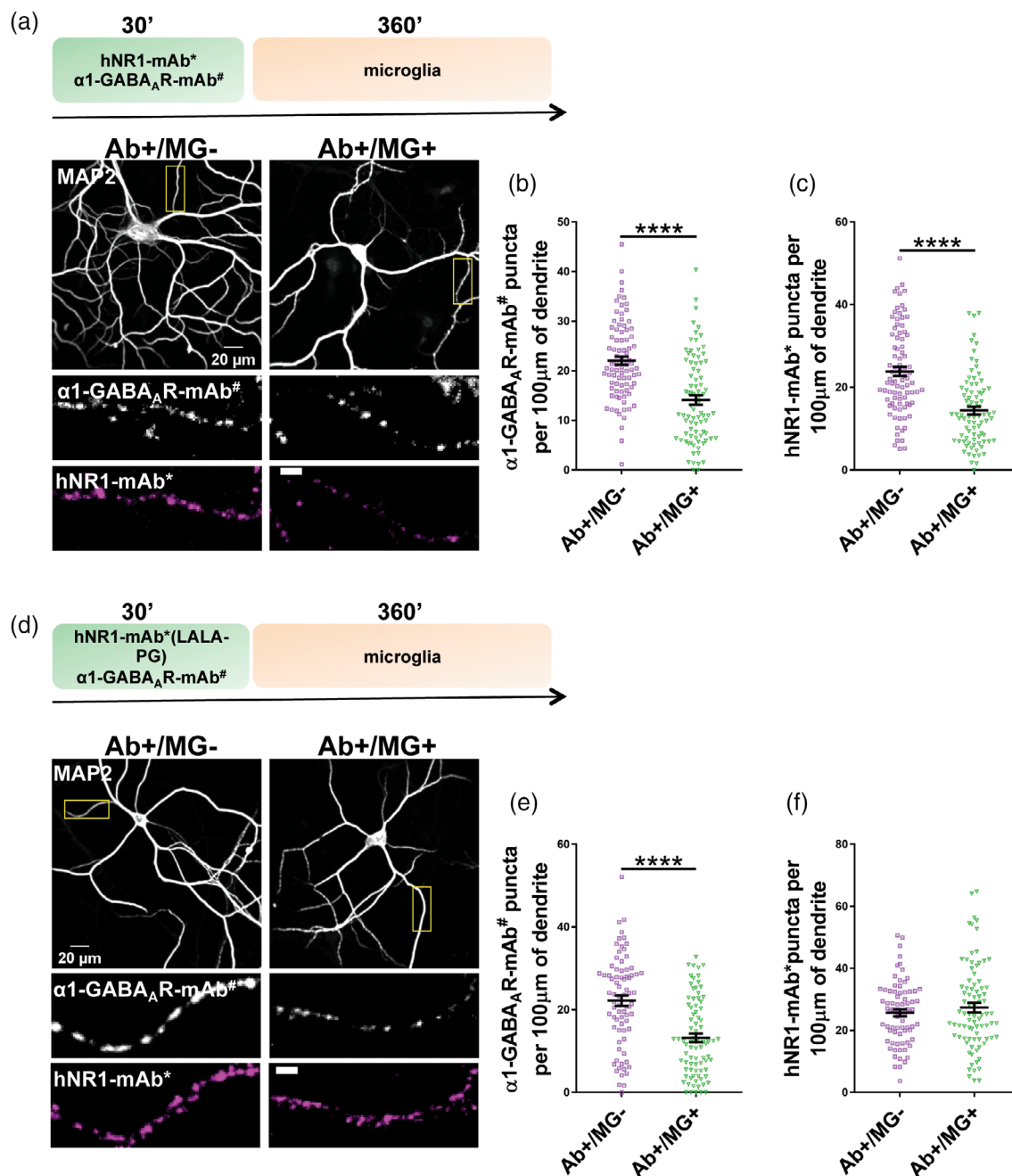


**FIGURE 10** Microglia mediates the selective removal of receptors bound by WT but not LALA-PG mutated autoantibodies. (a) Schematic depicting the experimental setup (upper panel). Representative images of MAP2 stained neurons (gray) bound with  $\alpha 1$ -GABA<sub>A</sub>R-mAb# (Alexa 594) and hNR1-mAb\* (Alexa 647) with (Ab+/MG+) or without (Ab+/MG-) microglia addition for 6 h. ROIs show  $\alpha 1$ -GABA<sub>A</sub>R-mAb# (white) and hNR1-mAb\* (magenta) puncta along dendritic segments. Scale bar, 5  $\mu$ m. (b and c) Quantification of  $\alpha 1$ -GABA<sub>A</sub>R-mAb# and hNR1-mAb\* puncta number per unit length of dendrite, respectively. The number of both was significantly reduced in the presence of microglia Ab+/MG+. Each data point represents an ROI from three independent experiments ( $n = 87$  for Ab+/MG-,  $n = 83$  for Ab+/MG+). Error bars represent SEM. Unpaired  $t$ -test was used to evaluate statistical significance (\*\*\*\*  $p < .00001$ ). (d) Schematic depicting the experimental setup (upper panel). Representative images of neurons with MAP2 staining (gray) with bound  $\alpha 1$ -GABA<sub>A</sub>R-mAb# (Alexa 594) and LALA-PG hNR1-mAb\* (Alexa 647) with or without microglia addition for 6 h. ROIs show  $\alpha 1$ -GABA<sub>A</sub>R-mAb# (white) and hNR1-mAb\* (magenta) puncta along dendritic segments. Scale bar, 5  $\mu$ m. (e and f) Quantitation of  $\alpha 1$ -GABA<sub>A</sub>R-mAb# and LALA-PG hNR1-mAb\* puncta number per unit length of dendrite, respectively.  $\alpha 1$ -GABA<sub>A</sub>R-mAb# number was reduced significantly in presence of microglia Ab+/MG+, with no change in the number of LALA-PG hNR1-mAb\* puncta along dendritic segments. Each data point represents an ROI from three independent experiments ( $n = 77$  for Ab+/MG-,  $n = 84$  for Ab+/MG+). Error bars represent SEM. Unpaired  $t$ -test was used to evaluate statistical significance (\*\*\*\*  $p < .00001$ ).

NMO-IgG was infused in to the spinal cord of mice, no motor impairment was observed when microglia were absent, but appeared around 5 days post ablation once microglia were allowed to replenish (T. Chen et al., 2020). Taken together, these studies highlight the relevance of autoantibody dependent FcγR and complement-driven activation of microglia and the associated downstream mechanisms in the etiology and pathology of specific autoimmune disorders.

At present it is less clear how and when such immune-mechanism manifest in patients with autoimmune encephalitis. Interestingly different antibody classes have been implicated, in for example, NMDAR autoimmune encephalitis, wherein IgG, IgA and IgM antibodies against NMDARs have all been isolated from sera of patients (Hara et al., 2018). Within the IgG subtype, IgG1 was reported to be the predominant subtype found in patients with NMDAR encephalitis (Tüzün et al., 2009). IgG1 and IgG3 subtypes have been shown to more efficiently trigger complement deposition as well as bind to different FcγRs expressed on the surface of myeloid cells and APCs (Dekkers et al., 2017; Vidarsson et al., 2014; Wang et al., 2018).

The recombinant hNR1-mAb used in this study belongs to the IgG1 subtype and can bind both to FcγRs and complement proteins like C1q (Figure S6c,d). By introducing point mutations described previously (LALA-PG, PA and LALA) (Lo et al., 2017; Saunders, 2019) into critical sites in the Fc region of hNR1-mAb, we could block its downstream interactions with FcγR1 and C1q complement protein. Surprisingly, we were unable to selectively dampen one interaction over the other as all three sets of mutations affected both FcγR1 and C1q binding (Figure S6c,d). This has been reported previously (Schlothauer et al., 2016) and could be due to partially overlapping binding regions of FcγRs and C1q (Vidarsson et al., 2014). Nonetheless, LALA-PG hNR1-mAb mutant was found to be highly effective in blocking both FcγR1 and C1q binding (Figure S6c,d). Importantly, blocking both FcγR1 and C1q binding and their subsequent downstream signaling, utilizing LALA-PG hNR1-mAb, prevented microglia-mediated loss of NMDAR puncta (Figure 7b,f) and synapses (Figure 8a–d) in our co-culture experiment. This suggests that NMDAR-bound hNR1-mAbs engage microglia using their Fc region either via FcγR and or complement binding leading to antibody dependent removal of NMDAR and synapses by microglia. Intriguingly, previous studies reported the lack of complement activation in patients with autoimmune encephalitis (Bien et al., 2012; Josep Dalmau et al., 2008; Tüzün et al., 2009). Although, these studies were performed on biopsied brain, one cannot rule out a role for complement at earlier phases of these diseases. Interestingly, all of these studies report prominent microgliosis in brains of these patients. Although there are obvious limitations of our *in-vitro* co-culture setup, as well as lack of specificity of our autoantibody Fc region mutants for complement vs FcγR, our data strongly indicate that engagement of autoantibodies via their Fc domains with complement and FcγR are critical interactions, promoting microglia-mediated removal of antibody labeled neurotransmitter receptors (e.g., NMDAR & GABA<sub>A</sub>R), concepts worth further investigation *in-vivo*.

In conclusion, our results argue that NMDAR/GABA<sub>A</sub>R autoantibodies can cause engagement of microglia, in addition to previously reported receptor crosslinking and internalization

(Hughes et al., 2010), promoting the loss of neurotransmitter receptors and synapses, thereby contributing to the etiology of autoantibody associated encephalitis symptoms and pathology. Further work is required to understand how autoantibody/receptor complexes lead to microglia activation and the associated release of inflammatory cytokines, which could in turn coordinate and recruit peripheral B cells, T cells and macrophages in sustaining and possibly worsening disease pathology. This study is an important step toward understanding this important yet poorly explored role of microglia in autoimmune encephalitis, as a common mechanism for disorders wherein pathogenic antibodies such as IgG1/ IgG3 subtypes are present, for example, in NMDAR and GABA<sub>A</sub>R encephalitis.

## AUTHOR CONTRIBUTIONS

Kazi Atikur Rahman, Ayub Boulos, Ewa Andrzejak, Craig C. Garner, and Aleksandra Ichkova designed research; Kazi Atikur Rahman, Marta Orlando and Ayub Boulos performed research; Kazi Atikur Rahman, Marta Orlando and Aleksandra Ichkova analyzed data; Harald Prüss provided the antibodies; Noam E. Ziv provided constructs; Kazi Atikur Rahman wrote the first draft of the paper; Kazi Atikur Rahman, Marta Orlando, Ewa Andrzejak, Ayub Boulos, Dietmar Schmitz, Noam E. Ziv, Craig C. Garner, Aleksandra Ichkova and Harald Prüss edited the paper; Kazi Atikur Rahman, Craig C. Garner and Aleksandra Ichkova wrote the paper. Craig C. Garner and Dietmar Schmitz acquired funding. The authors declare no competing financial interest.

## ACKNOWLEDGMENTS

This work was supported by the Einstein Foundation Berlin; by the German Center for Neurodegenerative Diseases; by the German Research Foundation Deutsche Forschungsgemeinschaft (DFG) (project 184695641—SFB 958 to C.C.G and D.S., project 327654276—SFB 1315 to D.S., project 415914819—FOR 3004 to D.S., project 431572356 to D.S., under Germany's Excellence Strategy—Exc-2049-390688087 to D.S. and C.C.G., PR1274/3-1, PR1274/4-1, PR1274/5-1 to H.P.); by the Helmholtz Association (HIL-A03 to H.P.); by the German Federal Ministry of Education and Research (BMBF) (Connect-Generate 01GM1908D to H.P., SmartAge—project 01GQ1420B to D.S.); and by the European Research Council (ERC) under the European Union's Horizon 2020 research and innovation program (Grant agreement No. 810580 to D.S.). We thank Sabina Tahirovic for her intellectual inputs, Jakob Kreye for his inputs, Thorsten Trimbuch and the Viral Core Facility of the Charité-Universitätsmedizin Berlin for cloning and production of viral constructs; Anny Kretschmer, Christine Bruns and Berit Söhl-Kielczynski for technical assistance; and the Advanced Medical Bioimaging Core Facility (AMBIO) of the Charité-Universitätsmedizin for support in acquisition of the light microscopy data and the Electron Microscopy Laboratory of the Institute of Integrative Neuroanatomy for granting us the access to their instruments.

## DATA AVAILABILITY STATEMENT

The data that support the findings of this study are available from the corresponding authors upon reasonable request.



## ORCID

Kazi Atikur Rahman  <https://orcid.org/0000-0001-8124-6026>

## REFERENCES

- Andrzejak, E., Rabinovitch, E., Kreye, J., Prüss, H., Rosenmund, C., Ziv, N. E., Garner, C. C., & Ackermann, F. (2022). Patient-derived anti-NMDA antibody disinhibits cortical neuronal networks through dysfunction of inhibitory neuron output. *The Journal of Neuroscience*, 42(15), 3253–3270. <https://doi.org/10.1523/JNEUROSCI.1689-21.2022>
- Banker, G., & Goslin, K. (1988). Developments in neuronal cell culture. *Nature*, 336(6195), 185–186. <https://doi.org/10.1038/336185a0>
- Barry, H., Hardiman, O., Healy, D. G., Keogan, M., Moroney, J., Molnar, P. P., Cotter, D. R., & Murphy, K. C. (2011). Anti-NMDA receptor encephalitis: An important differential diagnosis in psychosis. *The British Journal of Psychiatry*, 199(6), 508–509. <https://doi.org/10.1192/bjp.bp.111.092197>
- Behuet, S., Cremer, J. N., Cremer, M., Palomero-Gallagher, N., Zilles, K., & Amunts, K. (2019). Developmental changes of glutamate and GABA receptor densities in Wistar rats. *Frontiers in Neuroanatomy*, 13, 100. <https://doi.org/10.3389/fnana.2019.00100>
- Bien, C. G., Vincent, A., Barnett, M. H., Becker, A. J., Blümcke, I., Graus, F., Jellinger, K. A., Reuss, D. E., Ribalta, T., Schlegel, J., Sutton, I., Lassmann, H., & Bauer, J. (2012). Immunopathology of autoantibody-associated encephalides: Clues for pathogenesis. *Brain*, 135(5), 1622–1638. <https://doi.org/10.1093/brain/aws082>
- Bournazos, S., Wang, T. T., Dahan, R., Maamary, J., & Ravetch, J. V. (2017). Signaling by antibodies: Recent Progress. *Annual Review of Immunology*, 35, 285–311. <https://doi.org/10.1146/annurev-immunol-051116-052433>
- Camdessanché, J. P., Streichenberger, N., Cavillon, G., Rogemond, V., Jousserand, G., Honnorat, J., Convers, P., & Antoine, J. C. (2011). Brain immunohistopathological study in a patient with anti-NMDAR encephalitis. *European Journal of Neurology*, 18(6), 929–931. <https://doi.org/10.1111/j.1468-1331.2010.03180.x>
- Chen, A. K., Cheng, Z., Behlke, M. A., & Tsourkas, A. (2008). Assessing the sensitivity of commercially available fluorophores to the intracellular environment. *Analytical Chemistry*, 80(19), 7437–7444. <https://doi.org/10.1021/ac8011347>
- Chen, T., Lennon, V. A., Liu, Y. U., Bosco, D. B., Li, Y., Yi, M. H., Zhu, J., Wei, S., & Wu, L. J. (2020). Astrocyte-microglia interaction drives evolving neuromyelitis optica lesion. *The Journal of Clinical Investigation*, 130(8), 4025–4038. <https://doi.org/10.1172/jci134816>
- Coutinho, E., Menassa, D. A., Jacobson, L., West, S. J., Domingos, J., Moloney, T. C., Lang, B., Harrison, P. J., Bennett, D. L. H., Bannerman, D., & Vincent, A. (2017). Persistent microglial activation and synaptic loss with behavioral abnormalities in mouse offspring exposed to CASPR2-antibodies in utero. *Acta Neuropathologica*, 134(4), 567–583. <https://doi.org/10.1007/s00401-017-1751-5>
- Dalmau, J., Armangué, T., Planagumà, J., Radošević, M., Mannara, F., Leypoldt, F., Geis, C., Lancaster, E., Titulaer, M. J., Rosenfeld, M. R., & Graus, F. (2019). An update on anti-NMDA receptor encephalitis for neurologists and psychiatrists: Mechanisms and models. *The Lancet Neurology*, 18(11), 1045–1057. [https://doi.org/10.1016/S1474-4422\(19\)30244-3](https://doi.org/10.1016/S1474-4422(19)30244-3)
- Dalmau, J., Gleichman, A. J., Hughes, E. G., Rossi, J. E., Peng, X., Lai, M., Dessain, S. K., Rosenfeld, M. R., Balice-Gordon, R., & Lynch, D. R. (2008). Anti-NMDA-receptor encephalitis: Case series and analysis of the effects of antibodies. *The Lancet Neurology*, 7(12), 1091–1098. [https://doi.org/10.1016/S1474-4422\(08\)70224-2](https://doi.org/10.1016/S1474-4422(08)70224-2)
- Dalmau, J., & Graus, F. (2018). Antibody-mediated encephalitis. *The New England Journal of Medicine*, 378(9), 840–851. <https://doi.org/10.1056/NEJMra1708712>
- Dalmau, J., Tüzün, E., Wu, H. Y., Masjuan, J., Rossi, J. E., Voloschin, A., Baehring, J. M., Shimazaki, H., Koide, R., King, D., Mason, W., Sansing, L. H., Dichter, M. A., Rosenfeld, M. R., & Lynch, D. R. (2007). Paraneoplastic anti-N-methyl-D-aspartate receptor encephalitis associated with ovarian teratoma. *Annals of Neurology*, 61(1), 25–36. <https://doi.org/10.1002/ana.21050>
- Day, G. S., High, S. M., Cot, B., & Tang-Wai, D. F. (2011). Anti-NMDA-receptor encephalitis: Case report and literature review of an under-recognized condition. *Journal of General Internal Medicine*, 26(7), 811–816. <https://doi.org/10.1007/s11606-011-1641-9>
- Decker, H., Jürgensen, S., Adrover, M. F., Brito-Moreira, J., Bomfim, T. R., Klein, W. L., Epstein, A. L., De Felice, F. G., Jerusalinsky, D., & Ferreira, S. T. (2010). N-Methyl-D-aspartate receptors are required for synaptic targeting of Alzheimer's toxic amyloid- $\beta$  peptide oligomers. *Journal of Neurochemistry*, 115(6), 1520–1529. <https://doi.org/10.1111/j.1471-4159.2010.07058.x>
- Dekkers, G., Bentlage, A. E. H., Stegmann, T. C., Howie, H. L., Lissenberg-Thunnissen, S., Zimring, J., Rispens, T., & Vidarsson, G. (2017). Affinity of human IgG subclasses to mouse Fc gamma receptors. *MAbs*, 9(5), 767–773. <https://doi.org/10.1080/19420862.2017.1323159>
- Ehlers, M. D., Tingley, W. G., & Hagan, R. L. (1995). Regulated subcellular distribution of the NR1 subunit of the NMDA receptor. *Science*, 269(5231), 1734–1737. <https://doi.org/10.1126/science.7569904>
- Flach, A.-C., Litke, T., Strauss, J., Haberl, M., Gómez, C. C., Reindl, M., Saiz, A., Fehling, H.-J., Wienands, J., Odoardi, F., Lühder, F., & Flügel, A. (2016). Autoantibody-boosted T-cell reactivation in the target organ triggers manifestation of autoimmune CNS disease. *Proceedings of the National Academy of Sciences*, 113(12), 3323–3328. <https://doi.org/10.1073/pnas.1519608113>
- Fu, R., Shen, Q., Xu, P., Luo, J. J., & Tang, Y. (2014). Phagocytosis of microglia in the central nervous system diseases. *Molecular Neurobiology*, 49(3), 1422–1434. <https://doi.org/10.1007/s12035-013-8620-6>
- García-Serra, A., Radošević, M., Pupak, A., Brito, V., Ríos, J., Aguilar, E., Maudes, E., Ariño, H., Spatola, M., Mannara, F., Pedreño, M., Joubert, B., Ginés, S., Planagumà, J., & Dalmau, J. (2021). Placental transfer of NMDAR antibodies causes reversible alterations in mice. *Neurology Neuroimmunology Neuroinflammation*, 8(1), e915. <https://doi.org/10.1212/nxi.0000000000000915>
- Hara, M., Martínez-Hernández, E., Ariño, H., Armangué, T., Spatola, M., Petit-Pedrol, M., Saiz, A., Rosenfeld, M. R., Graus, F., & Dalmau, J. (2018). Clinical and pathogenic significance of IgG, IgA, and IgM antibodies against the NMDA receptor. *Neurology*, 90(16), e1386–e1394. <https://doi.org/10.1212/wnl.00000000000005329>
- Hinson, S. R., Clift, I. C., Luo, N., Kryzer, T. J., & Lennon, V. A. (2017). Autoantibody-induced internalization of CNS AQP4 water channel and EAAT2 glutamate transporter requires astrocytic Fc receptor. *Proceedings of the National Academy of Sciences of the United States of America*, 114(21), 5491–5496. <https://doi.org/10.1073/pnas.1701960114>
- Hong, S., Beja-Glasser, V. F., Nfonoyim, B. M., Frouin, A., Li, S., Ramakrishnan, S., Merry, K. M., Shi, Q., Rosenthal, A., Barres, B. A., Lemere, C. A., Selkoe, D. J., & Stevens, B. (2016). Complement and microglia mediate early synapse loss in Alzheimer mouse models. *Science*, 352(6286), 712–716. <https://doi.org/10.1126/science.1248373>
- Hovens, I. B., Nyakas, C., & Schoemaker, R. G. (2014). A novel method for evaluating microglial activation using ionized calcium-binding adaptor protein-1 staining: cell body to cell size ratio. *Neuroimmunology and Neuroinflammation*, 1, 82–88. <https://doi.org/10.4103/2347-8659.139719>
- Hughes, E. G., Peng, X., Gleichman, A. J., Lai, M., Zhou, L., Tsou, R., Parsons, T. D., Lynch, D. R., Dalmau, J., & Balice-Gordon, R. J. (2010). Cellular and synaptic mechanisms of anti-NMDA receptor encephalitis. *The Journal of Neuroscience*, 30(17), 5866–5875. <https://doi.org/10.1523/JNEUROSCI.0167-10.2010>
- Jézéquel, J., Johansson, E. M., Dupuis, J. P., Rogemond, V., Gréa, H., Kellermayer, B., Hamdani, N., Le Guen, E., Rabu, C., Lepleux, M.,



- Spatola, M., Mathias, E., Bouchet, D., Ramsey, A. J., Yolken, R. H., Tamouza, R., Dalmau, J., Honnorat, J., Leboyer, M., & Groc, L. (2017). Dynamic disorganization of synaptic NMDA receptors triggered by autoantibodies from psychotic patients. *Nature Communications*, 8(1), 1791. <https://doi.org/10.1038/s41467-017-01700-3>
- Ji, H., Ohmura, K., Mahmood, U., Lee, D. M., Hofhuis, F. M. A., Boackle, S. A., Takahashi, K., Holers, V. M., Walport, M., Gerard, C., Ezekowitz, A., Carroll, M. C., Brenner, M., Weissleder, R., Verbeek, J. S., Duchatelle, V., Degott, C., Benoist, C., & Mathis, D. (2002). Arthritis critically dependent on innate immune system players. *Immunity*, 16(2), 157–168. [https://doi.org/10.1016/S1074-7613\(02\)00275-3](https://doi.org/10.1016/S1074-7613(02)00275-3)
- Kinzel, S., Lehmann-Horn, K., Torke, S., Häusler, D., Winkler, A., Stadelmann, C., Payne, N., Feldmann, L., Saiz, A., Reindl, M., Lalive, P. H., Bernard, C. C., Brück, W., & Weber, M. S. (2016). Myelin-reactive antibodies initiate T cell-mediated CNS autoimmune disease by opsonization of endogenous antigen. *Acta Neuropathologica*, 132(1), 43–58. <https://doi.org/10.1007/s00401-016-1559-8>
- Koffie, R. M., Meyer-Luehmann, M., Hashimoto, T., Adams, K. W., Mielke, M. L., Garcia-Alloza, M., Micheva, K. D., Smith, S. J., Kim, M. L., Lee, V. M., Hyman, B. T., & Spires-Jones, T. L. (2009). Oligomeric amyloid beta associates with postsynaptic densities and correlates with excitatory synapse loss near senile plaques. *Proceedings of the National Academy of Sciences*, 106(10), 4012–4017. <https://doi.org/10.1073/pnas.0811698106>
- Kornau, H.-C., Kreye, J., Stumpf, A., Fukata, Y., Parthier, D., Sammons, R. P., Imbrosci, B., Kurpijweit, S., Kowski, A. B., Fukata, M., Prüss, H., & Schmitz, D. (2020). Human cerebrospinal fluid monoclonal LGI1 autoantibodies increase neuronal excitability. *Annals of Neurology*, 87(3), 405–418. <https://doi.org/10.1002/ana.25666>
- Kreye, J., Wenke, N. K., Chayka, M., Leubner, J., Murugan, R., Maier, N., Jurek, B., Ly, L. T., Brandl, D., Rost, B. R., Stumpf, A., Schulz, P., Radbruch, H., Hauser, A. E., Pache, F., Meisel, A., Harms, L., Paul, F., Dirnagl, U., ... Prüss, H. (2016). Human cerebrospinal fluid monoclonal N-methyl-D-aspartate receptor autoantibodies are sufficient for encephalitis pathogenesis. *Brain*, 139(10), 2641–2652. <https://doi.org/10.1093/brain/aww208>
- Kreye, J., Wright, S. K., van Casteren, A., Stöffler, L., Machule, M.-L., Reincke, S. M., Nikolaus, M., van Hoof, S., Sanchez-Sendin, E., Homeyer, M. A., Cordero Gómez, C., Kornau, H.-C., Schmitz, D., Kaindl, A. M., Boehm-Sturm, P., Mueller, S., Wilson, M. A., Upadhyay, M. A., Dhanger, D. R., ... Prüss, H. (2021). Encephalitis patient-derived monoclonal GABAA receptor antibodies cause epileptic seizures. *Journal of Experimental Medicine*, 218(11), e20210012. <https://doi.org/10.1084/jem.20210012>
- Krueger, S. R., Kolar, A., & Fitzsimonds, R. M. (2003). The presynaptic release apparatus is functional in the absence of dendritic contact and highly mobile within isolated axons. *Neuron*, 40(5), 945–957. [https://doi.org/10.1016/S0896-6273\(03\)00729-3](https://doi.org/10.1016/S0896-6273(03)00729-3)
- Lacor, P. N., Buniel, M. C., Chang, L., Fernandez, S. J., Gong, Y., Viola, K. L., Lambert, M. P., Velasco, P. T., Bigio, E. H., Finch, C. E., Krafft, G. A., & Klein, W. L. (2004). Synaptic targeting by alzheimer's-related amyloid  $\beta$  oligomers. *The Journal of Neuroscience*, 24(45), 10191–10200. <https://doi.org/10.1523/JNEUROSCI.3432-04.2004>
- Lee, S. H., Le Pichon, C. E., Adolfsson, O., Gafner, V., Pihlgren, M., Lin, H., Solanoy, H., Brendza, R., Ngu, H., Foreman, O., Chan, R., Ernst, J. A., DiCara, D., Hotzel, I., Srinivasan, K., Hansen, D. V., Atwal, J., Lu, Y., Bumbaca, D., ... Ayalon, G. (2016). Antibody-mediated targeting of tau in vivo does not require effector function and microglial engagement. *Cell Reports*, 16(6), 1690–1700. <https://doi.org/10.1016/j.celrep.2016.06.099>
- Li, S., Jin, M., Koeglperger, T., Shepardson, N. E., Shankar, G. M., & Selkoe, D. J. (2011). Soluble A $\beta$  oligomers inhibit long-term potentiation through a mechanism involving excessive activation of extrasynaptic NR2B-containing NMDA receptors. *The Journal of Neuroscience*, 31(18), 6627–6638. <https://doi.org/10.1523/JNEUROSCI.0203-11.2011>
- Liberman, L. D., & Liberman, M. C. (2015). Dynamics of cochlear synaptopathy after acoustic overexposure. *Journal of the Association for Research in Otolaryngology*, 16(2), 205–219. <https://doi.org/10.1007/s10162-015-0510-3>
- Lo, M., Kim, H. S., Tong, R. K., Bainbridge, T. W., Vernes, J. M., Zhang, Y., Lin, Y. L., Chung, S., Dennis, M. S., Zuchero, Y. J., Watts, R. J., Couch, J. A., Meng, Y. G., Atwal, J. K., Brezski, R. J., Spiess, C., & Ernst, J. A. (2017). Effector-attenuating substitutions that maintain antibody stability and reduce toxicity in mice. *The Journal of Biological Chemistry*, 292(9), 3900–3908. <https://doi.org/10.1074/jbc.M116.767749>
- Lois, C., Hong, E. J., Pease, S., Brown, E. J., & Baltimore, D. (2002). Germ-line transmission and tissue-specific expression of transgenes delivered by lentiviral vectors. *Science*, 295(5556), 868–872. <https://doi.org/10.1126/science.1067081>
- Lucchinetti, C. F., Guo, Y., Popescu, B. F. G., Fujihara, K., Itoyama, Y., & Misu, T. (2014). The pathology of an autoimmune astrocytopathy: Lessons learned from neuromyelitis optica. *Brain Pathology*, 24(1), 83–97. <https://doi.org/10.1111/bpa.12099>
- Ludwig, R. J., Vanhoorelbeke, K., Leypoldt, F., Kaya, Z., Bieber, K., McLachlan, S. M., Komorowski, L., Luo, J., Cabral-Marques, O., Hammers, C. M., Lindstrom, J. M., Lamprecht, P., Fischer, A., Riemekasten, G., Tersteeg, C., Sondermann, P., Rapoport, B., Wandinger, K.-P., Probst, C., ... Nimmerjahn, F. (2017). Mechanisms of autoantibody-induced pathology. *Frontiers in Immunology*, 8. <https://doi.org/10.3389/fimmu.2017.00603>
- Meberg, P. J., & Miller, M. W. (2003). Culturing hippocampal and cortical neurons. *Methods in Cell Biology*, 71, 111–127. [https://doi.org/10.1016/S0091-679X\(03\)01007-0](https://doi.org/10.1016/S0091-679X(03)01007-0)
- Meisslitzer-Ruppitsch, C., Röhl, C., Ranftler, C., Stangl, H., Neumüller, J., Pavelka, M., & Ellinger, A. (2013). Photooxidation technology for correlative light and electron microscopy. In D. J. Taatjes & J. Roth (Eds.), *Cell imaging techniques: Methods and protocols* (pp. 423–436). Humana Press.
- Moscato, E. H., Peng, X., Jain, A., Parsons, T. D., Dalmau, J., & Balice-Gordon, R. J. (2014). Acute mechanisms underlying antibody effects in anti-N-methyl-D-aspartate receptor encephalitis. *Annals of Neurology*, 76(1), 108–119. <https://doi.org/10.1002/ana.24195>
- Ohkawa, T., Fukata, Y., Yamasaki, M., Miyazaki, T., Yokoi, N., Takashima, H., Watanabe, M., Watanabe, O., & Fukata, M. (2013). Autoantibodies to epilepsy-related LGI1 in limbic encephalitis neutralize LGI1-ADAM22 interaction and reduce synaptic AMPA receptors. *The Journal of Neuroscience*, 33(46), 18161–18174. <https://doi.org/10.1523/JNEUROSCI.3506-13.2013>
- Paolicelli, R. C., Bolasco, G., Pagani, F., Maggi, L., Scianni, M., Panzanelli, P., Giustetto, M., Ferreira, T. A., Guiducci, E., Dumas, L., Ragozzino, D., & Gross, C. T. (2011). Synaptic pruning by microglia is necessary for normal brain development. *Science*, 333(6048), 1456–1458. <https://doi.org/10.1126/science.1202529>
- Pozzo, E. D., Tremolanti, C., Costa, B., Giacomelli, C., Milenkovic, V. M., Bader, S., Wetzel, C. H., Rupprecht, R., Taliani, S., Settimo, F. D., & Martini, C. (2019). Microglial pro-inflammatory and anti-inflammatory phenotypes are modulated by translocator protein activation. *International Journal of Molecular Sciences*, 20(18), 4467. <https://doi.org/10.3390/ijms20184467>
- Prüss, H. (2021). Autoantibodies in neurological disease. *Nature Reviews Immunology*, 21(12), 798–813. <https://doi.org/10.1038/s41577-021-00543-w>
- Rajendran, L., & Paolicelli, R. C. (2018). Microglia-mediated synapse loss in Alzheimer's disease. *The Journal of Neuroscience*, 38(12), 2911–2919. <https://doi.org/10.1523/JNEUROSCI.1136-17.2017>
- Rauschenberger, V., von Wardenburg, N., Schaefer, N., Ogino, K., Hirata, H., Lillesaar, C., Kluck, C. J., Meinck, H.-M., Borrmann, M.,



- Weishaupt, A., Doppler, K., Wickel, J., Geis, C., Sommer, C., & Villmann, C. (2020). Glycine receptor autoantibodies impair receptor function and induce motor dysfunction. *Annals of Neurology*, 88(3), 544–561. <https://doi.org/10.1002/ana.25832>
- Sabater, L., Giral, A., Boron, A., Hankiewicz, K., Blanco, Y., Llufrí, S., Alberch, J., Graus, F., & Saiz, A. (2009). Cytotoxic effect of neuromyelitis optica antibody (NMO-IgG) to astrocytes: an in vitro study. *Journal of Neuroimmunology*, 215(1–2), 31–35. <https://doi.org/10.1016/j.jneuroim.2009.07.014>
- Saio, K., & Glass, C. K. (2011). Microglial cell origin and phenotypes in health and disease. *Nature Reviews Immunology*, 11(11), 775–787. <https://doi.org/10.1038/nri3086>
- Saunders, K. O. (2019). Conceptual approaches to modulating antibody effector functions and circulation half-life. *Frontiers in Immunology*, 10, 1296. <https://doi.org/10.3389/fimmu.2019.01296>
- Schafer, D. P., Lehrman, E. K., Kautzman, A. G., Koyama, R., Mardinly, A. R., Yamasaki, R., Ransohoff, R. M., Greenberg, M. E., Barres, B. A., & Stevens, B. (2012). Microglia sculpt postnatal neural circuits in an activity and complement-dependent manner. *Neuron*, 74(4), 691–705. <https://doi.org/10.1016/j.neuron.2012.03.026>
- Schlothauer, T., Herter, S., Koller, C. F., Grau-Richards, S., Steinhart, V., Spick, C., Kubbies, M., Klein, C., Umaña, P., & Mössner, E. (2016). Novel human IgG1 and IgG4 Fc-engineered antibodies with completely abolished immune effector functions. *Protein Engineering, Design & Selection*, 29(10), 457–466. <https://doi.org/10.1093/protein/gzw040>
- Scott, A. M., Wolchok, J. D., & Old, L. J. (2012). Antibody therapy of cancer. *Nature Reviews Cancer*, 12(4), 278–287. <https://doi.org/10.1038/nrc3236>
- Smith, J. A., Das, A., Ray, S. K., & Banik, N. L. (2012). Role of pro-inflammatory cytokines released from microglia in neurodegenerative diseases. *Brain Research Bulletin*, 87(1), 10–20. <https://doi.org/10.1016/j.brainresbull.2011.10.004>
- Soltys, J., Liu, Y., Ritchie, A., Wemlinger, S., Schaller, K., Schumann, H., Owens, G. P., & Bennett, J. L. (2019). Membrane assembly of aquaporin-4 autoantibodies regulates classical complement activation in neuromyelitis optica. *The Journal of Clinical Investigation*, 129(5), 2000–2013. <https://doi.org/10.1172/jci122942>
- Tüzün, E., Zhou, L., Baehring, J. M., Bannykh, S., Rosenfeld, M. R., & Dalmau, J. (2009). Evidence for antibody-mediated pathogenesis in anti-NMDAR encephalitis associated with ovarian teratoma. *Acta Neuropathologica*, 118(6), 737. <https://doi.org/10.1007/s00401-009-0582-4>
- van Casteren, A. C. M., Ackermann, F., Rahman, K. A., Andrzejak, E., Rosenmund, C., Kreye, J., Prüss, H., Garner, C. C., & Ichkova, A. (2022). Differential modes of action of  $\alpha 1$ - and  $\alpha 1\gamma 2$ -autoantibodies derived from patients with GABAAR encephalitis. *Eneuro*, 9(6), 0369–22.2022. <https://doi.org/10.1523/eneuro.0369-22.2022>
- Vidarsson, G., Dekkers, G., & Rispen, T. (2014). IgG subclasses and allotypes: From structure to effector functions. *Frontiers in Immunology*, 5, 520. <https://doi.org/10.3389/fimmu.2014.00520>
- Walker, D. G., Tang, T. M., Mendsaikh, A., Tooyama, I., Serrano, G. E., Sue, L. I., Beach, T. G., & Lue, L.-F. (2020). Patterns of expression of purinergic receptor P2RY12, a putative marker for non-activated microglia, in aged and Alzheimer's disease brains. *International Journal of Molecular Sciences*, 21(2), 678.
- Wang, X., Mathieu, M., & Brezski, R. J. (2018). IgG Fc engineering to modulate antibody effector functions. *Protein & Cell*, 9(1), 63–73. <https://doi.org/10.1007/s13238-017-0473-8>
- Zhang, Z.-w., Peterson, M., & Liu, H. (2013). Essential role of postsynaptic NMDA receptors in developmental refinement of excitatory synapses. *Proceedings of the National Academy of Sciences*, 110(3), 1095–1100. <https://doi.org/10.1073/pnas.1212971110>
- Zhou, J., Tang, Z., Gao, S., Li, C., Feng, Y., & Zhou, X. (2020). Tumor-associated macrophages: Recent insights and therapies. *Frontiers in Oncology*, 10, 81–92. <https://doi.org/10.3389/fonc.2020.00188>
- Zuo, Y., & Deng, G.-M. (2021). Fc gamma receptors as regulators of bone destruction in inflammatory arthritis. *Frontiers in Immunology*, 12, 2500. <https://doi.org/10.3389/fimmu.2021.688201>

## SUPPORTING INFORMATION

Additional supporting information can be found online in the Supporting Information section at the end of this article.

**How to cite this article:** Rahman, K. A., Orlando, M., Boulos, A., Andrzejak, E., Schmitz, D., Ziv, N. E., Prüss, H., Garner, C. C., & Ichkova, A. (2023). Microglia actively remove NR1 autoantibody-bound NMDA receptors and associated post-synaptic proteins in neuron microglia co-cultures. *Glia*, 1–26. <https://doi.org/10.1002/glia.24369>